Theory of Slope Stability

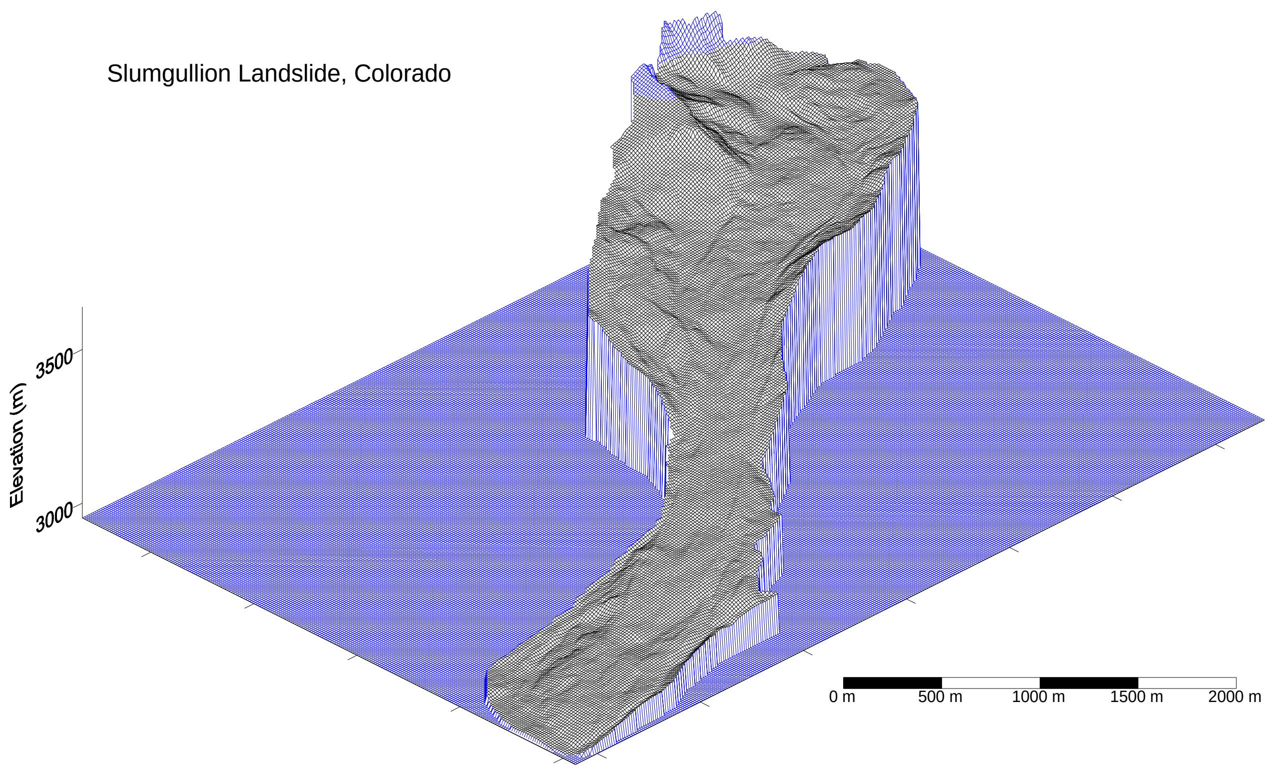

Prepared for

G 483/583 Anatomy of Landslides

(http://www.geol.pdx.edu/Courses/G483/)

by

Kenneth M. Cruikshank

Portland State University

Revision 1.30 (Spring Term 2002)

Based on course notes by

Arvid M. Johnson
Geo-Tesson Engineering Geology Laboratory
Purdue University

Table of Contents

List of Figures

List of Tables

List of Symbols

Symbol	Name	Use
ϕ	Phi	Angle of Internal friction of dry soil
$\overline{\phi}$		Angle of internal friction of saturated soil
$\overline{\phi}_r$		Residual angle of internal friction of saturated soil
$\overline{C}$		Cohesion of saturated soil
$\overline{C}_r$		Residual Cohesion of saturated soil
α	Alpha	Ground slope in Janbu analysis
C		Cohesion of dry soil
δ	Delta	Small increment
Δl		Length of slip surface in Janbu analysis
E		Magnitude of thrusting in Janbu analysis
F		Factor of safety. Defined as resisting forces / driving forces
γ	Gamma	Unit weight of dry soil
γ_s		Unit weight of solid particles
γ_t		Total unit weight material
γ_a		Unit weight of air
γ_w		Unit weight of water
$\overline{\gamma}$		Effective unit weight
η	Eta	Height of thrusting above slip surface in Janbu Analysis
h		Height of water table in Janbu analysis
φ	Phi	Slope of root with respect to shear zone
ϑ	Theta	Tangent to arc in methods of slices analysis
λ	Lambda	Coefficient in Morgenstern & Price stability analysis
N		Normal force
$\overline{N}$		Difference between water pressure and normal force (N–U)
θ	Theta	Slope angle
Θ	Theta	Volume fraction of solids (volume of solids / total volume)
σ	Sigma	Normal Stress on a slip surface
σ_{ij}		Components of the stress tensor
S		Shear force on slip surface
τ	Tau	Shear Stress on a slip surface
τ_f		Fraction of failure strength of soil in Janbu analysis
T		Shear force
t		Thickness of slide
t_c		Critical thickness of slide
u		Pore water pressure
U		Normal force exerted by pore water pressure on base of slice
W		Weight of an element
x		Horizontal distance to edge of slice in Janbu analysis (from toe)
y		Janbu: Height of slip surface (positive down from datum)
y		Infinite slope: Distance (“depth”) measured normal to slope
y_t		Height of line of thrusting in Janbu analysis
z		Height of ground surface in Janbu analysis

Some Definitions and Useful Conversion Factors

Stress ($ML^{-1}T^{-2}$): Force / Area. Common units are: Atmosphere, bar, Pascal, pounds/ft^2, pounds/in^2, inHg, dynes/cm^2

Force (MLT^{-2}): Mass times acceleration. Common units are: Newton (SI) and dyne (cgs).

Pascal. A measure of stress in SI units, defined as one Newton per meter-squared.

Newton. A measure of force in SI units. Defined as mass times acceleration. 1 Newton is the force required to accelerate 1 kg of mass at 1 m/s^2.

Dyne. A measure of force in cgs units. The force required to accelerate 1 gram at 1 cm/s^2.

Acceleration due to gravity: 9.806650 m/s^2, or 32.174048 ft/s^2.

Density of water (20°C): 0.99823 gm/ml (gm/cm^3) or 998.23 kg/m^3

Unit weight of water (20°C): 9789.2922 kg m^{-2} s^{-2} or 9.789 kN/m^3

Specific gravity: The ratio of the mass of a body to the mass of an equal volume of water at 4°C.

Unit conversions can be done using the CONVERT() function in Microsoft Excel, or the unit conversion functions in many calculators. You can also find numerous conversion factor sites on the World Wide Web. A nice book with all forms of conversion factors is:

Cook, J.L., 1991. *Conversion factors*. Oxford Science Publications, Oxford University Press, Oxford. 160 p.

From	Multiply "from" by	To
Atmosphere (atm)	$1.01 \times 10^5 \frac{\text{Pa}}{\text{atm}}$	Pascal (Pa)
Pascal (Pa)	$1 \frac{\text{N m}^{-2}}{\text{Pa}}$	N m^{-2}
Pascal (Pa)	$10^{-1} \frac{\text{dn cm}^{-2}}{\text{Pa}}$	dn cm^{-2} (dn = dyne)
psf (lb ft^{-2})	$47.88 \frac{\text{Pa}}{\text{psf}}$	Pascal (Pa)
psi (lb in^{-2})	$6.895 \times 10^3 \frac{\text{Pa}}{\text{psi}}$	Pascal (Pa)
pcf (lb ft^{-3})	$157.0875 \frac{\text{N m}^{-3}}{\text{pcf}}$	N m^{-3}
feet (ft)	$0.3048 \frac{\text{m}}{\text{ft}}$	meter (m)
pound (lb)	$4.448221 \frac{\text{N}}{\text{lb}}$	Newton (N)
pound (lb)	$0.453592 \frac{\text{kg}}{\text{lb}}$	Kilogram (kg)

Typical Material Values[1]

Description			Unit Weight (Saturated / Dry)		Friction Angle	Cohesion	
Type		*Material*	*Lb / ft^3*	*KN / m^3*	°	*Lb / ft^2*	*kPa*
Cohesionless	*Sand*	Loose sand, uniform grain size	118/90	19/14	18-34		
		Dense sand, uniform grain size	130/109	21/17	32-40		
		Loose sand, mixed grain size	124/99	20/16	34-40		
		Dense sand, mixed grain size	135/116	21/18	38-46		
	Gravel	Gravel, uniform grain size	140/130	22/20	34-37		
		Sand and gravel, mixed grain size	120/110	19/17	30-45		
	Blasted/broken rock	Basalt	140/110	22/17	40-50		
		Chalk	80/62	13/10	30-40		
		Granite	125/110	20/17	45-50		
		Limestone	120/100	19/16	35-40		
		Sandstone	110/80	17/13	35-45		
		Shale	125/100	20/16	30-35		
Cohesive	*Clay*	Soft bentonite	80/30	13/6	7-13	200 – 400	10 – 20
		Very soft organic clay	90/40	14/6	12-16	200 – 600	10 – 30
		Soft, slightly organic clay	100/60	16/10	22-27	400 – 1000	20 – 50
		Soft Glacial clay	110/76	17/12	27-32	600 – 1500	30 – 75
		Stiff glacial clay	130/105	20/17	30-32	1500 – 3000	75 – 150
		Glacial till, mixed grain size	145/130	23/20	32-35	3000 – 5000	150 – 250
	Rock	Hard igneous rocks Granite, basalt, porphyry	160 to 190	25 to 30	34-45	720000-1150000	35000-55000
		Metamorphic rocks Quartzite, gneiss, slate	160 to 180	25 to 28	30-40	400000-800000	20000-40000
		Hard sedimentary rocks Limestone, dolomite, sandstone	150 to 180	23 to 28	35-45	200000-600000	10000-30000
		Soft sedimentary rocks Sandstone, coal, chalk, shale	110 to 150	17 to 23	25-35	20000-400000	1000-20000

Higher friction angles in cohesionless materials occur at low confining or normal stresses

[1] from Hall 1994, Table 4D.1, p. 435

Summary of useful equations

Factor of Safety

Dry Infinite Slope

$$F = \frac{C + t\gamma\cos(\theta)\tan(\phi)}{t\gamma\sin(\theta)} \qquad (2.2.5a)$$

Submerged Infinite Slope

$$F = \frac{\overline{C} + t\,(\gamma_t - \gamma_w)\cos(\theta)\tan(\overline{\phi})}{t\,(\gamma_t - \gamma_w)\sin(\theta)} \qquad (2.3.11b)$$

Infinite Slope with Seepage parallel to slope

$$F = \frac{\overline{C} + t(\gamma_t - \gamma_w)\cos(\theta)\tan(\overline{\phi})}{t\gamma_t\sin(\theta)} \qquad (2.4.6a)$$

Infinite Slope with Seepage and Tree Roots

$$F = \frac{\overline{C} + \frac{1}{A}\sum_{i=1}^{n} F_i + t\,(\gamma_t - \gamma_w)\cos(\theta)\tan(\overline{\phi})}{t\,\gamma_t\sin(\theta)} \qquad (2.5.4a)$$

Fellenius method

$$F = \frac{\sum_{i=1}^{n}\left[\frac{b\,\delta x_i}{\cos(\vartheta_i)}\{\overline{C} - u_i\tan(\overline{\phi})\} + W_i\cos(\vartheta_i)\tan(\overline{\phi})\right]}{\sum_{i=1}^{n} W_i\sin(\vartheta_i)} \qquad (3.1.6)$$

Modified Bishop method

Use an initial guess for F in eq. (3.3.4) and use the resulting value for $\overline{N}_i$ in eq. (3.3.5). This will give you a new value of F to use in eq. (3.3.4). Continue iterating between these equations until F does not change.

$$\overline{N}_i = \frac{\frac{W_i}{\cos(\vartheta_i)} - U_i - b\,\frac{\delta x_i\sin(\vartheta_i)\,\overline{C}}{F\cos^2(\vartheta_i)}}{1 + \frac{\tan(\vartheta_i)\tan(\overline{\phi}_i)}{F}} \qquad (3.3.4)$$

$$F = \frac{\sum_{i=1}^{n} \left[\frac{b\ \delta x_i\ \bar{C}}{\cos(\vartheta_i)} + \bar{N} \tan(\bar{\phi}_i) \right]}{\sum_{i=1}^{n} W_i \sin(\vartheta_i)} \qquad (3.3.5)$$

Critical Thickness

Dry Infinite Slope

$$t_c = \frac{C}{\gamma \cos(\theta)\ [\tan(\theta) - \tan(\phi)]} \ ; \ F = 1 \qquad (2.2.5f)$$

Submerged Infinite Slope

$$t_c = \frac{\bar{C}}{(\gamma_t - \gamma_w) \cos(\theta)\ [\tan(\theta) - \tan(\bar{\phi})]} \ ; \ F = 1 \qquad (2.3.12)$$

Infinite Slope with Seepage parallel to slope

$$t_c = \frac{\bar{C}}{\gamma_t \cos(\theta)\ [\tan(\theta) - (1 - \gamma_w / \gamma_t) \tan(\bar{\phi})]} \ ; F = 1 \qquad (2.4.7)$$

Infinite Slope with Seepage and Tree Roots

$$t_c = \frac{\bar{C} + \frac{1}{A} \sum_{i=1}^{n} F_i}{\gamma_t \cos(\theta)\ [\tan(\theta) - (1 - \gamma_w / \gamma_t) \tan(\bar{\phi})]} \ ; F = 1 \qquad (2.5.4b)$$

Unit weight

$$\Theta = \frac{\text{Volume of Solids}}{\text{Total Volume}}$$

γ_a is the unit weight of air (taken to be 0 in 2.3.15b)
γ_s is unit weight of solid particles
γ_w is the unit weight of water

Dry soil

$$\gamma_t = \gamma_s\ \Theta + \gamma_a\ (1 - \Theta) \qquad (2.3.15a)$$

or

$$\gamma_t = \Theta\ \gamma_s \ ; \ \textit{Dry Soil} \qquad (2.3.\ 15b)$$

Mixture of water and solids

$$\gamma_t = \Theta\ \gamma_s + (1 - \Theta)\ \gamma_w \ ; \ \textit{Saturated Soil} \qquad (2.3.15c)$$

1. Theory of Slope Stability

In the lecture part of this course we will discuss a variety of methods of analysis of slope stability and instability. It is essential that the engineering geologist be intimately familiar with all of these methods because they provide ways of determining, relatively unambiguously, whether a given slope is likely to slide or whether it will remain stable. Perhaps most important, though, is that fact that the mechanical analysis of slope stability provides us with knowledge of what parameters control landsliding; the guesswork is entirely removed. At one time it was considered acceptable practice for the engineering geologist to make general statements about the effect of the geology, vegetation, the effect of intense rainfalls, or the effect of the facing direction of a slope (*e.g.*, north-facing slopes are less stable than south-facing slopes) on slope stability. No longer, though, is this acceptable. The engineering geologist is expected to know and understand theoretical and practical soil mechanics, better than the usual Civil Engineer, and nearly as well as the specialist, the Geotechnical Engineer. This course is designed to supplement the theory and practice of soil mechanics that you learn in courses taught in Civil Engineering. I assume that you have had at least one course in elementary soil mechanics. You certainly can complete this course without having had a course in soil mechanics, but I believe you will learn much more if you know some soil mechanics before you take this course.

With the availability of computers and slope analysis software there is now even less excuse for not doing the proper type of slope stability analysis. However, you cannot have computer programs do the thinking for you. The better you understand the mechanics of slope stability the more effective your use of these programs will be. In this class we will use some simple programs. The only difference between the programs we use and commercial programs is they are perhaps a little less user friendly, and do not produce a wide range of plots. Other than that, they are fully functional. You will get to see how little there is to slope stability!

It is well known in soil mechanics that three general types of parameters determine the stability or instability of a slope. One group concerns the *strength* of the soil. The strength includes cohesion, friction, interlocking of grains, reinforcement, for example by roots, and perhaps other factors. Another group concerns the *geometry* of the soil. This includes the shape of the ground surface, the shapes of possible slide surfaces, the pattern of layering within the soil, and the forms of significant discontinuities such as joints or shear zones. The other group of parameters relates to the *pore-water pressure*. These include the pore-water pressure itself as well as the seepage forces set up by movement of water through the soil. Our approach is going to be to keep certain parameters constant and to investigate effects of the remaining parameters. In this way we can understand effects of the various parameters. Thus, we will perform a series of investigations in which we assume that the slope has simple geometry and is very long. These theoretical investigations allow us to assess effects of certain idealized pore-water pressure distributions and effects of tree roots on slope stability. Then we will assume that the failure surface is a segment of a circle, so that we can readily treat landslides where the thickness of the sliding debris is a significant fraction of the distance from the head to the toe of the landslide mass. Finally we will introduce rather complicated and accurate methods of stability analysis that require the use of a computer. These more complicate methods allow us to treat most problems of slope stability.

2. Infinite Slope

2.1 Equilibrium equations

The simplest problem of slope stability that we can analyze, and that we should understand in detail because it is so basic, is that of the stability of the so-called infinite slope. The infinite slope solution is also an exact solution, the methods of slices which we examine later are approximate solutions. In an infinite slope solution we determine the conditions under which a layer of soil of thickness *t* will slip along a surface, *a*-*a*', that is parallel to the ground surface, which has a slope angle of θ. The cross section of the infinite slope is shown in Figure 1. At this point you should study relevant pages in Lambe & Whitman (1969, §13.9, p. 191-193 & Chapter 14, p. 352-373), Turner & Schuster (1996, Chapter 13, p. 337), Budhu [, 2000 #5090, §11.6, p. 592], or Abramson *et al.* (1996, §6.6, p. 352). We will use a somewhat different procedure from that presented by some of the texts above, but I hope that the two approaches will increase your understanding, rather than confuse you. Several of the texts above deal with a vertical distance, *d*, rather than with the thickness, *t*, of the sliding body, but one can readily convert from one to the other with the relation,

$$t = d\cos(\theta) \qquad (2.1.1)$$

Using the vertical distance makes the final equations look more complex.

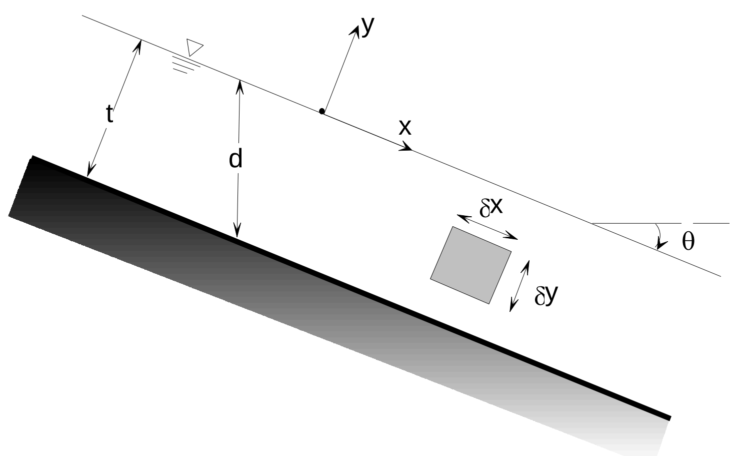

Figure 1. Definition diagram for infinite slope analysis

The way we will approach this problem is to select a tiny element of soil, with dimensions δ*x* and δ*y* (in the plane of the figure), and unit weight[2], γ, where the coordinates are selected to be parallel or normal to the ground surface. Let the element have a dimension δ*z* normal to the view in Figure 1. Then, for static equilibrium of forces, *F*, and moments, *M*, must sum to zero,

$$\Sigma M = 0\ ;\quad \Sigma F_x = 0\ ;\quad \Sigma F_y = 0 \qquad (2.1.2)$$

[2] *Unit weight*, γ, is density times acceleration due to gravity (*g*), so that it has units of force per unit of volume (*e.g.*, N/m^3). Often you will see stresses reported in units of kg/cm^2 in soil mechanics literature. This is nonsense. However, merely replace kg/cm^2 by atmospheres and you will be dealing with a proper quantity (see conversion tables on p. iv).

The stresses acting on the tiny element are shown in Figure 2a, whereas the forces are shown in Figure 2b. The forces, of course, are the stresses multiplied by the areas on which the stresses act. The stresses vary across the width or depth of the element, and the different stresses on opposite sides are indicated by primed and un-primed values. For example, σ_{xx} is the normal stress acting on the left-hand side of the element and σ'_{xx} is the normal stress acting on the right-hand side:

$$\sigma'_{xx} = \sigma_{xx} + \frac{\partial \sigma_{xx}}{\partial x}\ \delta x \qquad (2.1.3a)$$

Similarly,

$$\sigma'_{xy} = \sigma_{xy} + \frac{\partial \sigma_{xy}}{\partial x}\ \delta x \qquad (2.1.3b)$$

$$\sigma'_{yx} = \sigma_{yx} + \frac{\partial \sigma_{yx}}{\partial y}\ \delta y \qquad (2.1.3c)$$

$$\sigma'_{yy} = \sigma_{yy} + \frac{\partial \sigma_{yy}}{\partial y}\ \delta y \qquad (2.1.3d)$$

Note that all the stresses shown in Figure 2A are shown in their *positive* directions, so that normal stresses are positive if compressive.

As already stated, the forces, *N* and *T*, are equal to the corresponding stresses times the appropriate areas. Thus,

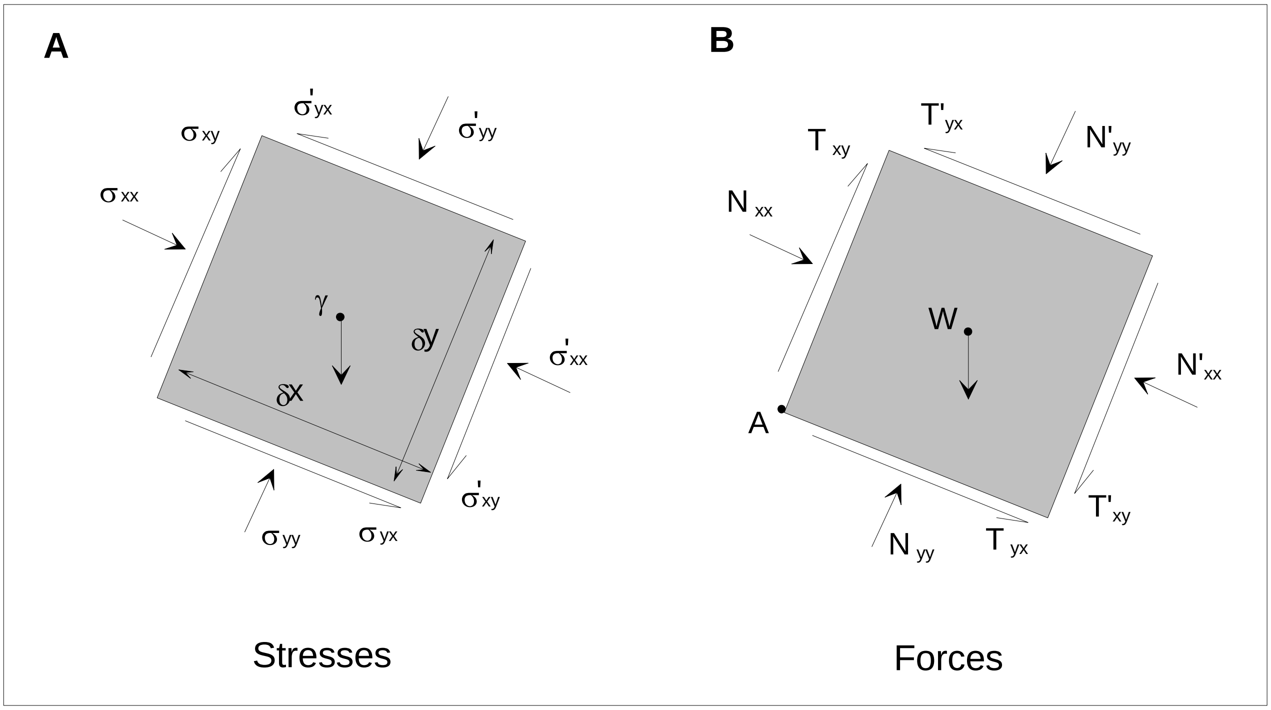

Figure 2. Unit element in a slide mass. Note that all the stresses shown are in their *positive* directions, so that normal stresses are positive if compressive.

$$N_{xx} = \sigma_{xx}\, \delta y\, \delta z \quad ; \quad N'_{xx} = \sigma'_{xx}\, \delta y\, \delta z \tag{2.1.4a}$$

$$T_{xy} = \sigma_{xy}\, \delta y\, \delta z \quad ; \quad T'_{xy} = \sigma'_{xy}\, \delta y\, \delta z \tag{2.1.4b}$$

$$T_{yx} = \sigma_{yx}\, \delta x\, \delta z \quad ; \quad T'_{yx} = \sigma'_{yx}\, \delta x\, \delta z \tag{2.1.4c}$$

$$N_{yy} = \sigma_{yy}\, \delta x\, \delta z \quad ; \quad N'_{yy} = \sigma'_{yy}\, \delta x\, \delta z \tag{2.1.4d}$$

So much for definitions.

Now let us apply the equations of moment and force equilibrium, eqs. (2.1.2). Summing moments about the lower left-hand corner (point *A*) in the element shown in Figure 2B, with counter-clockwise being a positive moment,

$$T'_{yx}\, \delta y - T'_{xy}\, \delta x - (N_{xx} - N'_{xx})\, \frac{\delta y}{2} + (N_{yy} - N'_{yy})\, \frac{\delta x}{2} - \gamma\, (\delta x\, \delta y\, \delta z) \left[\frac{\delta x}{2} \cos(\theta) + \frac{\delta y}{2} \sin(\theta) \right] = 0 \tag{2.1.5a}$$

in which the weight of the element, *W*, is

$$W = \gamma\, (\delta x\, \delta y\, \delta z) \tag{2.1.5b}$$

The lever arms for T_{yx} and T_{xy} are zero. Substituting eqs. (2.1.3) into (2.1.4) and the resulting eqs. (2.1.4) into the result above,

$$\begin{aligned} &(\sigma_{yx} + \frac{\partial \sigma_{yx}}{\partial y}\, \delta y)\, (\delta y\, \delta x\, \delta z) - (\sigma_{xy} + \frac{\partial \sigma_{xy}}{\partial x}\, \delta x)\, (\delta y\, \delta x\, \delta z) \\ &+ \frac{\partial \sigma_{xx}}{\partial x} \frac{\delta x}{2}\, (\delta y\, \delta x\, \delta z) - \frac{\partial \sigma_{yy}}{\partial y} \frac{\delta y}{2}\, (\delta y\, \delta x\, \delta z) \\ &- \gamma\, (\delta y\, \delta x\, \delta z)\, (\frac{\delta x}{2} \cos(\theta) + \frac{\delta y}{2} \sin(\theta)) = 0 \end{aligned} \tag{2.1.5c}$$

Now, dividing each term in eq. (2.1.5c) by the volume of the element ($\delta x\, \delta y\, \delta z$), and taking the limit of the resulting eq. (2.1.5c) as $\delta x \to 0$ and $\delta y \to 0$, we derive the result that the moments sum to zero if

$$\sigma_{yx} - \sigma_{xy} = 0 \tag{2.1.6a}$$

$$\sigma_{yx} = \sigma_{xy} \tag{2.1.6b}$$

Summing forces in the *x*- and *y*-directions we derive the equilibrium equations in terms of stresses. Thus, summing forces in the *x*-direction

$$\Sigma F_x = N_{xx} - N'_{xx} + T_{yx} - T'_{yx} + W \sin(\theta) = 0 \tag{2.1.7a}$$

Substituting eqs. (2.1.3) into (2.1.4) and the resulting eqs. (2.1.4) into (2.1.7a)

$$\sigma_{xx}\, \delta y \delta z - \left(\sigma_{xx} + \frac{\partial \sigma_{xx}}{\partial x}\, \delta x \right) \delta y \delta z + \sigma_{yx}\, \delta x \delta z - \left(\sigma_{yx} + \frac{\partial \sigma_{yx}}{\partial x}\, \delta y \right) \delta x \delta z + \gamma\, (\delta y\, \delta x\, \delta z) \sin(\theta) = 0 \tag{2.1.7b}$$

and then dividing by the volume of the element,

$$\frac{\sigma_{xx}}{\delta x} - \frac{\sigma_{xx}}{\delta x} - \frac{\partial\sigma_{xx}}{\partial x} + \frac{\sigma_{yx}}{\delta y} - \frac{\sigma_{yx}}{\delta y} - \frac{\partial\sigma_{yx}}{\partial x} + \gamma \sin(\theta) = 0, \tag{2.1.7c}$$

which leaves

$$\frac{\partial\sigma_{xx}}{\partial x} + \frac{\partial\sigma_{yx}}{\partial y} = \gamma \sin(\theta) \tag{2.1.7d}$$

Similarly, summing forces in the *y*-direction,

$$N_{yy} - N'_{yy} - W\cos(\theta) + T_{xy} - T'_{xy} = 0 \tag{2.1.8a}$$

so that, proceeding as before, we derive

$$\frac{\partial\sigma_{yy}}{\partial y} + \frac{\partial\sigma_{xy}}{\partial x} = -\gamma \cos(\theta) \tag{2.1.8b}$$

Equations (2.1.7d & 2.1.8b) are the *equilibrium equations*, in terms of stresses.

Now, for problems involving infinite slopes, the stresses cannot change in the *x*-direction. Therefore, eqs. (2.1.7d & 2.1.8b) can be written as total differential equations,

$$\frac{\mathrm{d}\sigma_{yx}}{\mathrm{d}y} = \gamma \sin(\theta) \tag{2.1.9a}$$

$$\frac{\mathrm{d}\sigma_{yy}}{\mathrm{d}y} = -\gamma \cos(\theta) \tag{2.1.9b}$$

From equation 2.1.5b we should also note that

$$\frac{\mathrm{d}\sigma_{yx}}{\mathrm{d}y} = \frac{\mathrm{d}\sigma_{xy}}{\mathrm{d}y} \tag{2.1.10}$$

Integrating eqs. (2.1.7), we derive,

$$\sigma_{xy} = y\,\gamma \sin(\theta) + C_0 \tag{2.1.11a}$$

$$\sigma_{yy} = -y\,\gamma \cos(\theta) + C_1 \tag{2.1.11b}$$

in which C_0 and C_1 are arbitrary constants. However, the shear stress and normal stress are necessarily zero at the ground surface, so that the constants are zero,

$$\sigma_{xy} = y\,\gamma \sin(\theta) \tag{2.1.12a}$$

$$\sigma_{yy} = -y\,\gamma\cos(\theta) \tag{2.1.12b}$$

We should note that we have made no assumption concerning the rheological properties of the material in the slope. Thus eqs. (2.1.12) are valid whether the material is soil, water, lava or some other material. However, to say anything about slope stability, we will need to introduce the rheological properties of the soil.

The simple relationships in eqs. 2.1.12 represent the equilibrium conditions in any material. The material is out of equilibrium when these conditions are not satisfied. The question in slope stability is how far out of equilibrium is the slope, and in what direction is out of equilibrium – is it stable or unstable?

2.2 Dry Soil

Let us first consider the stability of a slope underlain by dry soil, so that pore-water pressures are zero. For dry soil, one generally assumes that the soil shears when the shear stress is equal to the shear strength of the soil. A very simple model of shear strength, which works remarkably well for most soils, is Coulomb's law of friction[3],

$$\textit{strength in shear} = C + \sigma \tan(\phi) \tag{2.2.1}$$

in which C is cohesion, σ is normal stress acting across the surface of shearing, and ϕ is the angle of internal friction (generally about 30° for sand and 15° to 25° for clay, see table on p. v). We generally state the strength in terms of a yield condition, which is

$$|\tau| \leq C + \sigma \tan(\phi) \tag{2.2.2}$$

in which τ is the shear stress acting on the surface of failure in shear. The absolute value sign is required because the shear strength equally resists positive or negative shear stress. The "less-than-or-equal", ≤, symbol indicates that the shear stress applied to the soil must be less than or equal to the shear strength of the soil; this is by definition shear strength.

Furthermore, we generally compute a *factor of safety* against sliding, F, where the factor of safety is a measure of the closeness to conditions of sliding that exist in a slope. The factor of safety is defined as the ratio of the shear strength to the actual shear stress,

$$F = \frac{C + \sigma \tan(\phi)}{|\tau|} \tag{2.2.3}$$

The factor of safety is greater-than one if the shear strength is greater than the shear stress, so that the slope is stable, and it is equal to one if failure is impending. If you compute a factor of safety less-than one, get out of the way!

Let us compute the factor of safety for an infinite slope. The shear stress is maximal at the bottom of the soil (2.1.12a, Figure 1), where $y = -t$, so that from eq. (2.12),

$$\sigma_{xy} = -t\,\gamma \sin(\theta) \tag{2.2.4a}$$

$$\sigma_{yy} = t\,\gamma \cos(\theta) \tag{2.2.4b}$$

For stability we are interested in the shear stress on planes normal to the y-axes, so that

$$\tau = \sigma_{xy} = -t\,\gamma \sin(\theta) \tag{2.2.4c}$$

The normal stress acting on this plane is σ_{yy} , so that

$$\sigma = \sigma_{yy} = t\,\gamma \cos(\theta) \tag{2.2.4d}$$

Accordingly, the expression for the factor of safety against sliding, eq. (2.2.3), becomes,

$$F = \frac{C + t\,\gamma \cos(\theta) \tan(\phi)}{t\,\gamma \sin(\theta)} \quad ; \textit{dry soil} \tag{2.2.5a}$$

[3] Also called *Mohr-Coulomb* Law in some texts, such as Lamb & Whitman (1969, Chapter 11, p. 137)

If the cohesion, C, were zero,

$$F = \frac{\tan(\phi)}{\tan(\theta)} \quad ;\ dry\ soil\ ; \quad C = 0 \qquad (2.2.5b)$$ [4]

Equation (2.2.5b) represents a common notion for the angle of internal friction. If we let the factor of safety be one then eq. (2.2.5b) becomes

$$\tan(\theta) = \tan(\phi) \quad \text{or} \quad \phi = \theta \qquad (2.2.5c)$$

Thus if a cohesionless material was piled into a cone, the angle of the cone will be the angle of internal friction for the material. This is not an accurate measure of ϕ. ϕ is determined from triaxial tests and a Mohr diagram.

Further, if the thickness of the potential slide is equal to the critical thickness for sliding, the factor of safety is one. In this case we can solve for the critical thickness by setting F = l in eq. (2.2.5a),

$$1 = \frac{C + t\,\gamma \cos(\theta) \tan(\phi)}{t\,\gamma \sin(\theta)} \qquad (2.2.5d)$$

$$t\,\gamma \sin(\theta) = C + t\,\gamma \cos(\theta) \tan(\phi) \qquad (2.2.5e)$$

$$t_c = \frac{C}{\gamma \cos(\theta)\,[\tan(\theta) - \tan(\phi)]} \quad ;\ F = 1\ ; \quad dry\ soil \qquad (2.2.5f)$$

since $\tan(\theta) = \sin(\theta)/\cos(\theta)$. The critical thickness, t_c, is zero if the cohesion is zero. This may appear to be a surprising result.

At this point you should complete exercise 1 (p. 39).

2.3 Infinite slope in standing body of water

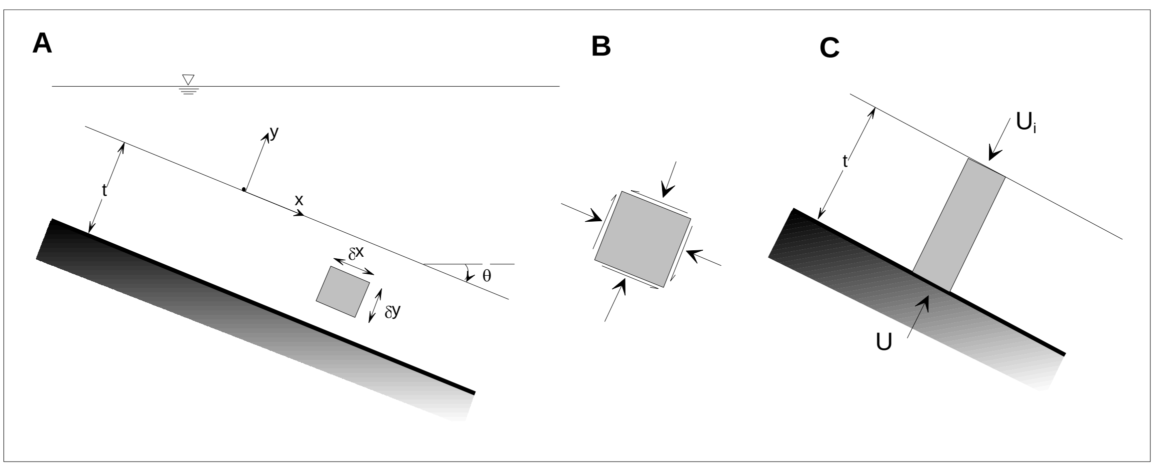

Figure 3. Definition diagram for a submerged infinite slope.

[4] This is the equation at the top right-hand side of p. 193 of Lambe and Whitman (1969).

The next problem that we will consider is the infinite slope that is submerged by a standing body of water (Lambe & Whitman 1969, §24.1, p. 352). Now I realize that this is a physical impossibility, but it is possible for a very long slope to be submerged and our analysis will be approximately valid for such a slope, and will be very accurate as long as the length of the slope is, say, ten or more times the thickness of the sliding debris. The water and soil is a two-phase system, which must be considered explicitly in our analysis. Also, we should follow Terzaghi and use "effective stress" concept of soil strength. This is one of the most important concepts in soil mechanics (see Lambe 1969, chapter 10, p. 241). According to the concept of effective stress, the strength of the soil is

$$\textit{strength in shear} = \overline{C} + (\sigma - u)\tan(\overline{\phi}) \qquad (2.3.1)$$

where $\overline{C}$ and $\overline{\phi}$ are material properties of the *saturated soil*, and u is pore-water pressure. As before, σ is the normal stress on a potential surface of failure.

The body of water is not moving, so we can compute the water pressure everywhere within the system:

$$\frac{\partial u}{\partial x} = \gamma_w \sin(\theta) \qquad (2.3.2a)$$ [5]

$$\frac{\partial u}{\partial y} = -\gamma_w \cos(\theta) \qquad (2.3.2b)$$

Where γ_w is the unit weight of water. Integrating eq. (2.3.2b),

$$u = -y\,\gamma_w \cos(\theta) + f(x) \qquad (2.3.3a)$$

where $f(x)$ is a function of x. Substituting (2.3.3a) into eq. (2.3.2a) we derive

$$\frac{\partial}{\partial x}\{-y\,\gamma_w \cos(\theta) + f(x)\} = \frac{\mathrm{d}\,f(x)}{\mathrm{d}x} = \gamma_w \sin(\theta) \qquad (2.3.3b)$$

(because y, of course, is independent of x), so that

$$f(x) = x\,\gamma_w \sin(\theta) + C_o \qquad (2.3.3c)$$

in which C_o is a constant. Thus eq. (2.3.3a) becomes,

$$u = \gamma_w (x \sin(\theta) - y\cos(\theta)) + C_o \qquad (2.3.3d)$$

Now, let the water pressure at the surface of the soil mass, at $y = 0$, be u_i.

$$u_i = \gamma_w\ x \sin(\theta) + C_o \qquad (2.3.4a)$$

$$C_o = u_i - \gamma_w\ x\sin(\theta) \qquad (2.3.4b)$$

Then we can write eq. (2.3.3d) in the final form,

$$u = \gamma_w (x \sin(\theta) - y\cos(\theta)) + u_i - \gamma_w\ x\sin(\theta) \qquad (2.3.5a)$$

$$u = -y\,\gamma_w \cos(\theta) + u_i. \qquad (2.3.5b)$$

---

[5] Note that we derived eqs. (2.3.2), another form of equilibrium equations, by inspection of eqs.(2.1.7d, 2.1.8b). Water will not support shear if it is stationary.

Thus we have derived an expression for the pore-water pressure within the soil mass, as well as the water pressure within the standing body of water overlying the soil mass.

At this point we return to the equations for the stresses within the soil mass, eqs. (2.1.7d, 2.1.8b). Those equations are for the total stresses, and are a result of the combined density of the soil and the water contained in the soil. Thus, instead of using dry unit weight, γ, we use total unit weight, γ_t[6] of the soil, and eqs. (2.1.7d, 2.1.8b) become

$$\frac{\partial \sigma_{xx}}{\partial x} + \frac{\partial \sigma_{yx}}{\partial y} = \gamma_t \sin(\theta) \qquad (2.3.6a)$$

$$\frac{\partial \sigma_{yy}}{\partial y} + \frac{\partial \sigma_{xy}}{\partial x} = -\gamma_t \cos(\theta) \qquad (2.3.6b)$$

However, the shear stress is independent of *x*, so that the second term in eq. (2.3.6b) is zero. The normal stress σ_{xx} varies with *x* only because the pore-water pressure, *u*, varies with *x* in the manner indicated in eq. (2.3.3d).

$$\frac{\partial \sigma_{xx}}{\partial x} + \frac{\partial \sigma_{yx}}{\partial y} = \gamma_t \sin(\theta) \qquad (2.3.7a)$$

$\partial \sigma_{xx}/\partial x$ varies according to equation (2.3.3d). The reason for this is as you move in the *x*-direction you are moving deeper, thus the pressure (σ_{xx}) is increasing. This can be seen by examining Figure 3. The pore-water pressure change can be written

$$\frac{\partial \sigma_{xx}}{\partial x} = \lim_{\delta x \to 0} \frac{u_{x+\delta x} - u_x}{\delta x} \qquad (2.3.7b)$$

or

$$\frac{\partial \sigma_{xx}}{\partial x} = \frac{\gamma_w [(x + \delta x) \sin(\theta) - y \cos(\theta)] + C_o - \gamma_w [x \sin(\theta) - y \cos(\theta)] - C_o}{\delta x} \qquad (2.3.7c)$$

$$\frac{\partial \sigma_{xx}}{\partial x} = \gamma_w \sin(\theta) \qquad (2.3.7d)$$

Thus, using eq. (2.3.7d), eqs. (2.3.6a); become,

$$\gamma_w \sin(\theta) + \frac{d\sigma_{yx}}{dy} = \gamma_t \sin(\theta) \qquad (2.3.8a)$$

or

$$\frac{d\sigma_{yx}}{dy} = (\gamma_t - \gamma_w) \sin(\theta) \qquad (2.3.8b)$$

$$\frac{\partial \sigma_{yy}}{\partial y} = -\gamma_t \cos(\theta) \qquad (2.3.8c)$$

[6] The total specific weight is not simply the addition of the unit weight of solids plus the unit weight of water. We have to allow for the porosity of the material. See equations 2.3.15 at the end of this section.

The component of σ_{xx} that comes from the soil will be a constant (as with the dry soil derivation). $\partial\sigma_{yy}/\partial y$ is left as a partial derivative since σ_{yy} varies with both *x* and *y* (again, this can be seen from examining Figure 3). You should compare these equations with eq. (2.1.9).

We should note two features of eqs. (2.3.8b,c). The normal stress depends upon the unit weight of the mixture of solids and water, whereas the shear stress depends upon the buoyant unit weight, $(\gamma_t - \gamma_w)$, of the mixture. Further, we have made no special assumptions in deriving eqs. (2.3.8b,c). A special assumption is introduced only in a following step, when we assume that eq. (2.3.1) describes adequately the strength of the soil.

Integrating eqs. (2.3.8b,c),

$$\sigma_{yx} = \sigma_{xy} = y\,(\gamma_t - \gamma_w)\sin(\theta) \qquad (2.3.9a)$$

in which the arbitrary constant was set equal to zero, because the shear stress is zero for $y = 0$. Further,

$$\sigma_{yy} = -\,y\,\gamma_t \cos(\theta) + g(x) \qquad (2.3.9b)$$

Where $g(x)$ is an arbitrary function of *x*. However, at $y = 0$, $\sigma_{yy} = u_i$, eq. (2.3.5), so that

$$\sigma_{yy} = -\,y\,\gamma_t \cos(\theta) + u_i \qquad (2.3.9c)$$

in which

$$u_i = \gamma_w\, x \sin(\theta) + C_i \qquad (2.3.9d)$$

where C_i is a constant, which we need not determine, as we will show below.

Next we consider the possibility of sliding of a soil mass of thickness *t* (Fig. 3A). The shear stress parallel to the base is

$$\tau = \left|\sigma_{xy}\right| = \left|-\,t\,(\gamma_t - \gamma_w)\sin(\theta)\right| \qquad (2.3.10a)$$

and the effective normal stress at the base, $y = -t$, is (eq. (2.3.9b) minus (2.3.5b)),

$$\sigma - u = \sigma_{yy} - u = t\,(\gamma_t - \gamma_w)\cos(\theta) \qquad (2.3.10b)$$

The factor of safety against sliding is

$$F = \frac{\overline{C} + (\sigma - u)\tan(\overline{\phi})}{\left|\tau\right|} \qquad (2.3.11a)$$

so that,

$$F = \frac{\overline{C} + t\,(\gamma_t - \gamma_w)\cos(\theta)\tan(\overline{\phi})}{t\,(\gamma_t - \gamma_w)\sin(\theta)} \quad ;\ \textit{Submerged slope} \qquad (2.3.11b)$$

The critical thickness, t_c, derived for a factor of safety of one, is

$$t_c = \frac{\overline{C}}{(\gamma_t - \gamma_w)\cos(\theta)\,[\tan(\theta) - \tan(\overline{\phi})]} \quad ;\ F = 1 \qquad (2.3.12)$$

If the cohesion is negligible, the factor of safety reduces to that of a dry slope,

$$F = \frac{\tan(\bar{\phi})}{\tan(\theta)} \;;\; \bar{C} = 0 \qquad (2.3.13)$$

as noted by Lambe and Whitman (1969). We would note, further, that the critical thickness for sliding (as well as the factor of safety) is increased for the submerged slope relative to a dry slope, *if the strengths are unchanged*[7]. This somewhat surprising result can be explained as follows:

Let Θ be the volume fraction of solids in a soil.

$$\Theta = \frac{\text{Volume of Solids}}{\text{Total Volume}} \qquad (2.3.14)$$

For the dry soil, therefore, the total unit weight, γ_t, which we called γ in previous paragraphs, is

$$\gamma_t = \gamma_s\,\Theta + \gamma_a\,(1 - \Theta) \qquad (2.3.15a)$$

in which γ_a is the unit weight of air and γ_s is unit weight of solid particles. Let the unit weight of air be effectively zero, so that eq. (2.3.15a) simplifies to

$$\gamma_t = \Theta\,\gamma_s \;;\; \textit{Dry Soil} \qquad (2.3.15b)$$

On the other hand, the total unit weight of the mixture of water and solids is,

$$\gamma_t = \Theta\,\gamma_s + (1 - \Theta)\,\gamma_w \;;\; \textit{Saturated Soil} \qquad (2.3.15c)$$

Therefore, the effective unit weight of saturated soil is

$$\bar{\gamma} = \gamma_t - \gamma_w = \Theta\,(\gamma_s - \gamma_w) \qquad (2.3.15d)$$

Clearly the effective unit weight, eq. (2.3.15d), used in the computation of factor of safety and critical thickness, eqs. (2.3.11b) and (2.3.12), is always less than the unit weight for dry soil, eq. (2.3.15b). Thus the statement by Lambe & Whitman (1969), that the factor of safety is unchanged by submergence, is correct for the special case of $C = 0$. The factor of safety is increased, however, if $C \neq 0$, and $C = \bar{C}$, $\bar{\phi} = \phi$.

Time for another exercise! This time do exercise 2 (p. 40).

2.4 Infinite slope with seepage parallel to the slope

Thus far we have considered a slope underlain by dry soil, so that the pore-water pressure was zero, and a slope completely submerged in a standing body of water. Water is one of the most important factors in landsliding. It is usually an increase in water content that will initiate and maintain landslide movement. The importance of water, especially infiltration has been discussed at some length in the literature (e.g., Baum & Reid 1995).

Now we will consider the stability of a slope where the water table is at the ground surface and where equipotential lines are normal to the ground surface (see Lambe1969, p. 354). It is beyond the scope of this course to compute the pore-water pressure distribution within the soil

---

[7] We will expect some changes in strength parameters when the material is saturated (See *Progress of consolidation in delta front and prodelta clays of the Mississippi River*, by B. McClelland in *Marine Géotechnique*).

under these conditions, so we will use results presented by Lambe & Whitman (1969, p. 354, fig. 24.3):

$$u = -\,y\,\gamma_w \cos(\theta) \tag{2.4.1}$$

Perhaps you find it interesting that this is the same as eq. (2.3.5b) with u_i, the pore-water pressure at the ground surface, equal to zero. If so, maybe you should try to figure it out. It really is relatively simple. The pore-water pressure is independent of x, so that eqs. (2.3.6) reduce to

$$\frac{d\sigma_{yx}}{dy} = \gamma_t \sin(\theta) \tag{2.4.2a}$$

$$\frac{d\sigma_{yy}}{dy} = -\,\gamma_t \cos(\theta) \tag{2.4.2b}$$

Integrating, and using the boundary conditions that the normal and shear stresses are zero at the ground surface, $y = 0$, we derive,

$$\sigma_{yx} = y\,\gamma_t \sin(\theta) \tag{2.4.3a}$$

$$\sigma_{yy} = -\,y\,\gamma_t \cos(\theta) \tag{2.4.3b}$$

As before, we assume that failure is occurring or potentially could occur at a depth $y = -\,t$, so that the shear and normal stresses there are,

$$\tau = -\,t\,\gamma_t \sin(\theta) \tag{2.4.4a}$$

$$\sigma = t\,\gamma_t \cos(\theta) \tag{2.4.4b}$$

The factor of safety against sliding is

$$F = \frac{\bar{C} + (\sigma - u)\tan(\bar{\phi})}{|\tau|} \tag{2.4.5}$$

so that, using eq. (2.4.1),

$$F = \frac{\bar{C} + t\,(\gamma_t - \gamma_w)\cos(\theta)\tan(\bar{\phi})}{t\,\gamma_t \sin(\theta)} \quad ;\ \textit{Seepage parallel to slope} \tag{2.4.6a}$$

and if the cohesion is zero,

$$F = \frac{[1 - (\gamma_w/\gamma_t)\,]\tan(\bar{\phi})}{\tan(\theta)} \quad ;\ \bar{C} = 0 \tag{2.4.6b}$$

This is the same as writing

$$F = \frac{\tan(\bar{\phi})}{\tan(\theta)} - \frac{\gamma_w}{\gamma_t}\,\frac{\tan(\bar{\phi})}{\tan(\theta)}$$

Thus the factor of safety is reduced by γ_w/γ_t compared with the equivalent dry slope.

The critical thickness, corresponding to a factor of safety of one, is

$$t_c = \frac{\overline{C}}{\gamma_t \cos(\theta)\ \{\tan(\theta) - (1 - \gamma_w / \gamma_t) \tan(\overline{\phi})\}} \ ; F = 1 \qquad (2.4.7)$$

Therefore, the condition of seepage parallel to the surface is the least stable condition of the slope; the factor of safety against sliding and the critical thickness are least for this condition.

Time for yet another exercise! Now complete exercise 3 (p. 40).

2.5 Incorporation of strength controlled by tree roots

Mary Riestenberg (Riestenberg & Sovonick-Dunford 1983) has done research into the effect of roots of woody vegetation on the stability of colluvium on steep slopes. Independently, the same results had been derived by Waldron (1977), Wu *et al*. (1979) and Wu & Swanston (1989).

For a small slide that she studied in detail, Mary found that the average shear strength contributed by the roots was about 5.7 kN/m^2 of the shear surface, whereas the average strength contributed by residual friction, alone, was about 0.7 kN/m. The tree roots, therefore, increased the factor of safety against sliding 9-fold, in this case. Based on observations of many landslides of various thicknesses in the Cincinnati area, Mary has tentatively concluded that tree roots can significantly increase the resistance to sliding for soil masses up to about two meters thick. Here we will briefly review her theoretical analysis, in order to determine the effect of tree roots on resistance to sliding for very long slopes. Further data on root strength is given by Turner (in Turner & Schuster 1996, p. 538, tables 20-1 & 20-2) and Hall *et al*. (1994, p. 543).

Figure 4 shows normal, F_n, and tangential, F_s, forces contributed at the failure surface at the instant a tree root is ready to break in tension. The force required to break the tree root is F. Thus,

$$F_s = F \sin(\varphi) \qquad (2.5.1a)$$

$$F_n = F \cos(\varphi) \qquad (2.5.1b)$$

where φ is the angle of inclination of the tree root (Figure 4).

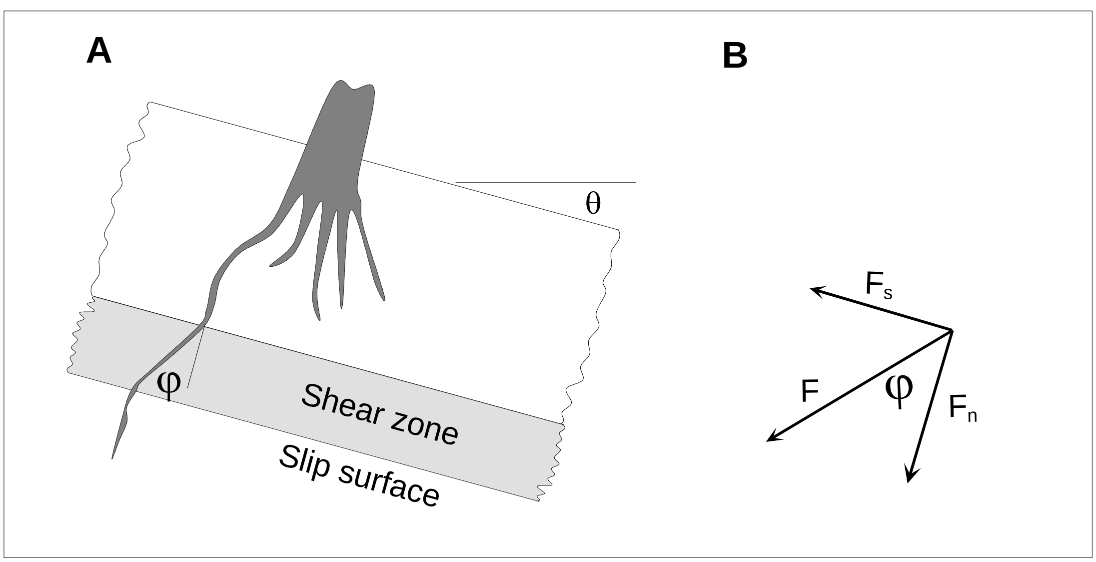

Figure 4. Role of tree roots in reinforcing a soil mass.

Now the average normal stress applied to the surface of failure by the tree roots is

$$\sigma = \frac{1}{A} \sum_{i=1}^{n} F_i \cos(\varphi_i) \tag{2.5.2a}$$

in which A is the area of the part of the slip surface penetrated by a total of n roots, F_i is the force required to break each root, and φ_i is angle of inclination of each root. Similarly, the average tangential stress for the same unit of area, A, is

$$\tau = \frac{1}{A} \sum_{i=1}^{n} F_i \sin(\varphi_i) \tag{2.5.2b}$$

where, again, the sum is taken over all the roots that penetrate that certain area of the slip surface.

The average strength contributed by tree roots is to the shear resistance of the material

$$\tau_r = \sigma \tan(\overline{\phi}) + \tau \tag{2.5.3a}$$

$$\tau_r = \frac{1}{A} \sum_{i=1}^{n} F_i \left[\cos(\varphi_i) \tan(\overline{\phi}) + \sin(\varphi_i)\right] \tag{2.5.3b}$$

In order to perform a stability analysis, we add this strength, eq. (2.4.3b), to that contributed by the soil without roots, eq. (2.3.1). Mary noted, however, the roots that penetrated the slip surface in the small landslide complex that she studied had become distorted from a nearly vertical orientation to an orientation nearly parallel to the slip surface. In this case, $\varphi_i \cong 90°$ and eq. (2.4.3b) simplifies to

$$\tau_r = \frac{1}{A} \sum_{i=1}^{n} F_i \tag{2.5.3c}$$

since *cos*(90°) = 0, and *sin*(90°) = 1.

A further justification for using the form (2.5.3c) is that the quantity in brackets in eq. (2.5.3b) maximizes where

$$\mathrm{Cot}(\varphi) = \tan \overline{\phi} \tag{2.5.3d}$$

that is,

$$(\varphi_i)_{\text{max resistance}} = 90° - \overline{\phi}. \tag{2.5.3e}$$

Therefore, if the angle of internal friction is 10°, φ is 80°, and in this case (2.5.3b) is a close approximation to eq 2.5.3c.

Adding the strength contributed by the tree roots, eq. (2.5.2c), to that contributed by the soil without roots, eq. (2.3.1), we derive

$$F = \frac{\overline{C} + \frac{1}{A}\sum_{i=1}^{n} F_i + t(\gamma_t - \gamma_w)\cos(\theta)\tan(\overline{\phi})}{t\gamma_t \sin(\theta)} \tag{2.5.4a}$$

for the factor of safety, and

$$t_c = \frac{\overline{C} + \frac{1}{A}\sum_{i=1}^{n} F_i}{\gamma_t \cos(\theta)\,[\tan(\theta) - (1 - \gamma_w / \gamma_t)\tan(\overline{\phi})]} \;;\; F = 1 \qquad (2.5.4b)$$

for the critical thickness.

Mary determined tensile strengths of roots sampled from the base of the landslide that she studied, and the results are presented in fig. 12 of her M.S. thesis (Riestenberg 1981), in terms of force (in Newtons) required to break a root of a certain diameter (in mm). For example, for woody roots about 2 mm in diameter, the force required to break the roots in tension ranges from about 100 to 200 Newtons. The table below summarizes some of her measurements.

Table 1. Summary of root strength data for live sugar maples. From Riestenberg (1981, fig. 12).

Root Diameter (mm)	Breaking Force (*F*, Newtons)	
2	100 – 200	100*
5	250 – 450	450*
10	900 – 1500	1,500*
30	7,000 – 2,0000	10,000*

* Indicates best estimates of strengths.

In order to use eqs. (2.5.4) for stability analysis, of course, you must be able to measure or estimate the number of roots of various sizes that penetrate a given area of the slip surface. This, unfortunately, is difficult to do in practice.

Now complete exercise 4 (p. 41).

3. Method of slices

3.1 Introduction

In following paragraphs we will derive the equations essential for understanding two methods of slope-stability analysis, the Fellenius and the modified-Bishop methods. We will not discuss how one computes pore-water pressures along slip surfaces, nor will be discuss how one determines relevant soil properties to use in the analyses. For discussions of these subjects, please see Lambe & Whitman (1969). In particular, you should learn something about the construction of flow nets in analysis of flow of ground water (e.g., Fetter 1994, Freeze & Cherry 1979), and you should be familiar with residual and peak strengths of clayey soils (e.g., Skempton 1964).

Both the Fellenius and the modified-Bishop methods are examples of a group of methods called *method of slices*. In these methods, a possible slip surface, with the form of a segment of a circular cylinder, is assumed, and the driving and resisting moments are computed in order to determine the factor of safety against sliding. The factor of safety is defined as

$$F = \sum_{i=1}^{n} M_r \Big/ \sum_{i=1}^{n} M_d \qquad (3.1.1)$$

that is, it is the ratio of the sum of the resisting moments to the sum of the driving moments. In cross section the circular cylinder projects as a segment of a circle (Figure 5). The mass of soil contained between the circular arc (*ABC*) and the ground surface is divided into a series of slices, the sides of which are vertical (Figure 5A). The number of slices is somewhat arbitrary, but different numbers should be selected and factors of safety computed in order to find the number above which the factor of safety is changed insignificantly by increasing the number of slices. In Figure 5A we have arbitrarily selected nine slices of various widths.

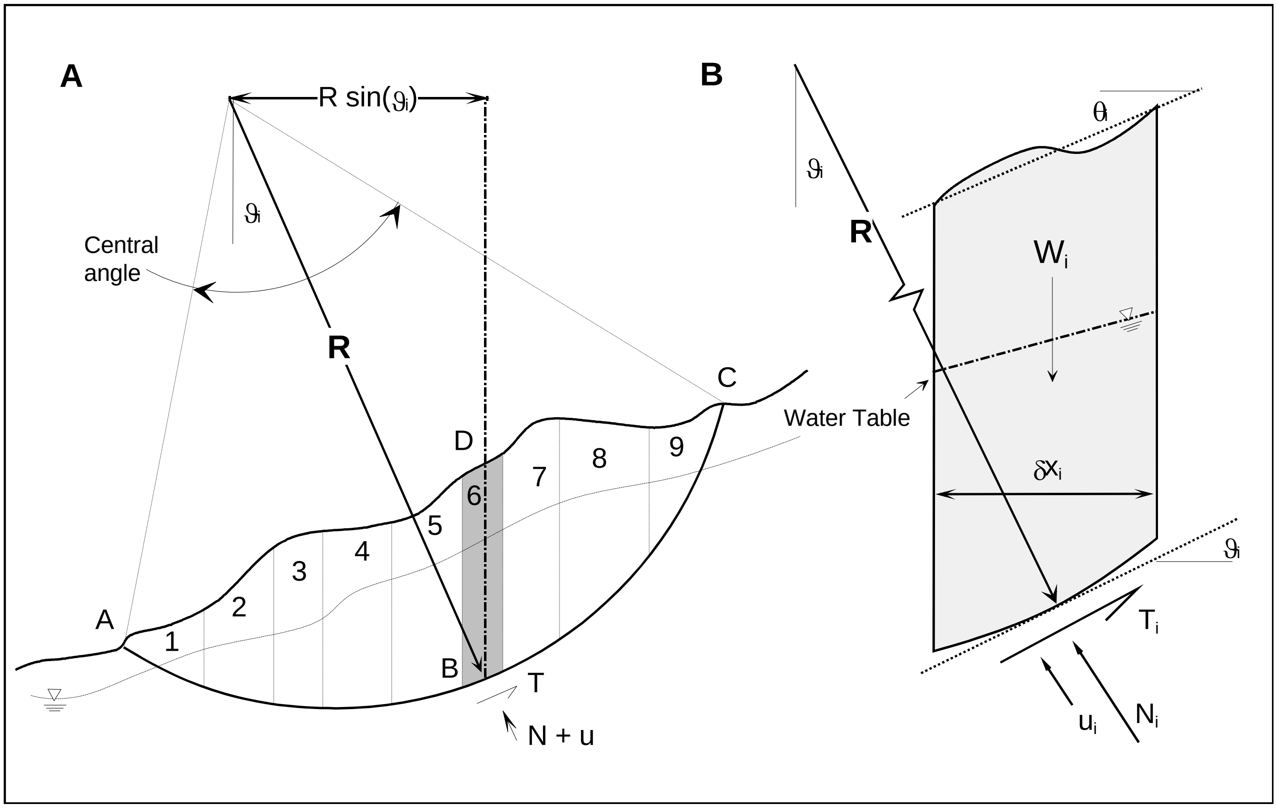

Figure 5. Definition diagram for Fellenius and Bishop methods. A simple slip surface is assumed, and the total moments are determined by summing moments for each slice. The factor of safety is defined as the ratio of the sum of the resisting moments divided by the sum of the driving moments.

After selecting the slices, we compute resisting and driving moments. One slice, the sixth shown in Figure 5A, is shown in Figure 5B as a free-body diagram of a typical slice. The free-body diagram shows all relevant forces and moments acting on the element. One force shown is *W*, the weight of the slice. It is determined by multiplying the area of the slice times the unit of breadth in the direction normal to the page, times the unit weight of the soil. However, in this example we must use the unit weight for unsaturated soil above the water table, and the saturated unit weight for the part of the slice below the water table. Another force is the shear force, T_i, which, in both the Fellenius and the modified-Bishop methods, is given by the Terzaghi-Coulomb failure criterion,

$$\tau_i = \overline{C} + (\sigma - u)\tan(\overline{\phi}) \tag{3.1.2a}$$

or

$$T_i = \frac{\overline{C}_i\, b\, \delta x_i}{\cos(\vartheta_i)} + \left(N_i - \frac{u_i\, b\, \delta x_i}{\cos(\vartheta_i)}\right)\tan(\overline{\phi}_i) \tag{3.1.2b}$$

in which b is unit breadth (one meter or one foot, depending upon the system of units for the constants), δx_i is the width of the slice measured horizontally (Figure 5B), ϑ is the slope angle of the tangent to the bottom of the slice, N is the total force normal to the slip surface, and u is the pore-water pressure at the base of the slice. Thus the quantity $\{b\ \delta x_i / \cos(\vartheta_i)\}$ is the area over which a stress is acting.

The normal force, N, acts through the center of the circle, so that its lever arm is zero, and it exerts a zero moment with respect to the center. The shear force, T has a lever arm equal to the radius of the circle, so that the moment resisting sliding for that slice simply is,

$$R\ T_i \tag{3.1.3a}$$

Therefore, the total resisting moment is

$$\sum_{i=1}^{n} M_r = R\ T_i \tag{3.1.3b}$$

where T_i is given by eq. (3.1.2b).

The driving moment arises entirely from the weight of the slice. The lever arm for a slice is $R \sin(\vartheta_i)$. You can verify this by examining Figure 5A, where the lever arm for slice 6 is illustrated. You should verify that the angle between the vertical and the radius for slice i is equal to θ_i and that the slope to the tangent to the base of slice i is equal to ϑ_i, the same angle. Thus the driving moment for slice i is

$$R\ W_i \sin(\vartheta_i) \tag{3.1.4}$$

and the sum of the driving moments is

$$\sum_{i=1}^{n} M_d = R \sum_{i=1}^{n} W_i \sin(\vartheta_i) \tag{3.1.5}$$

Substituting eq. (3.1.2b) into (3.1.3b), and the resulting eq. (3.1.3b) as well as (3.1.5) into (3.1.1), we derive the expression for the factor of safety,

$$F = \frac{\sum_{i=1}^{n}\left[\frac{b\ \delta x_i}{\cos(\vartheta_i)}\{\overline{C} - u_i \tan(\overline{\phi})\} + N_i \tan(\overline{\phi})\right]}{\sum_{i=1}^{n} W_i \sin(\vartheta_i)} \tag{3.1.6}$$

in which the sums are to be taken over all the slices.

Equation (3.1.6) is used for both the Fellenius and the modified-Bishop methods of stability analysis. The differences in the two methods are entirely a result of the way the normal force, N_i, is defined. It is important to recognize that neither method of analysis satisfies force equilibrium. This is an approximation to the true solution. There was no such approximation made in the infinite slope analysis.

3.2 Fellenius Method

Perhaps the most widely used method of stability analysis is the Fellenius, method, sometimes called the Swedish Circle Method. In this method, the normal force on each slice is *assumed* to be equal to the vertical component of the weight of that slice,

$$N_i = W_i \cos(\vartheta_i) \tag{3.2.1}$$

Thus we merely substitute eq. (3.2.1) into (3.1.6) and proceed to solve problems.

Whitman & Bailey (1967, p. 486) point out that the fundamental assumption in the Fellenius method is that the resultant of all forces acting on the sides of an element (these forces are not even shown in Figure 5B) act parallel to the force T_i. Thus, these side forces do not enter into the expression for N, given in eq. (3.2.1). In general, these side forces will contribute to N, in which case eq. (3.2.1) will be in error. According to Whitman & Bailey (1967), factors of safety computed by the Fellenius method can be seriously in error. One source of error, they indicate, is the manner in which pore-water pressures generally are introduced into the analysis. Another source of error is a result of error in the computed values of N. They state that the error increases with an increase in the central angle (Figure 5A) of the failure arc; the error results from underestimating the value of N along steeply sloping parts of the failure arc. In order to minimize errors due to pore-water pressures, Whitman suggests using the buoyant unit weight of the slices if the pore-water is static (for details, see 1967, p. 491).

3.3 Modified Bishop Method

In the modified Bishop method of stability analysis, the method of computing N is different. In this method we sum forces in the vertical direction, so that, for each slice,

$$W_i = N_i \cos(\vartheta_i) + T_i \sin(\vartheta_i) \tag{3.3.1}$$

in which T_i is the shear force that is mobilized, the shear strength of the soil, divided by the factor of safety, F:

$$T_i = \frac{\dfrac{b\,\delta x_i}{\cos(\vartheta_i)}\bar{C} + (N_i - U_i)\tan(\bar{\phi})}{F} \tag{3.3.2a}$$

in which

$$U_i = \frac{u_i\, b\,\delta x_i}{\cos(\vartheta_i)} \tag{3.3.2b}$$

is the normal force exerted by the pore-water on the base of the slice, as in eq. (3.1.2b).

Let

$$\bar{N}_i = N_i - U_i \tag{3.3.2c}$$

then eq. (3.3.1) becomes

$$W_i = (\bar{N}_i + U_i)\cos(\vartheta_i) + T_i \sin(\vartheta_i) \tag{3.3.3}$$

Substituting eq. (3.3.2a) into (3.3.3) and solving for $\bar{N}_i$

$$\bar{N}_i = \frac{\dfrac{W_i}{\cos(\vartheta_i)} - U_i - b\,\dfrac{\delta x_i \sin(\vartheta_i)\,\bar{C}}{F\cos^2(\vartheta_i)}}{1 + \dfrac{\tan(\vartheta_i)\tan(\bar{\phi}_i)}{F}} \tag{3.3.4}$$

Rewriting eq. (3.1.7) using eq. (3.3.2c),

$$F = \frac{\displaystyle\sum_{i=1}^{n}\left[\frac{b\,\delta x_i\,\bar{C}}{\cos(\vartheta_i)} + \bar{N}_i \tan(\bar{\phi}_i)\right]}{\displaystyle\sum_{i=1}^{n} W_i \sin(\vartheta_i)} \tag{3.3.5}$$

In order to compute the factor of safety, we substitute eq. (3.3.4) into eq. (3.3.5). The factor of safety occurs on both sides of the equal sign, and cannot be explicitly solved for, so we solve eqs. (3.3.4) and (3.3.5) by iteration. That is, we guess F and then compute N_i. Then we use those values to obtain an improved estimate of F with eq. (3.3.5). We then use this new estimate of F to compute N_i and then again solve for F using eq. (3.3.5). We repeat this procedure until the factor of safety changes by insignificant amounts.

Whitman & Bailey (1967) indicate that a fundamental assumption in the modified Bishop method is that the resultant of forces acting on the sides of elements (such forces are not even shown in Figure 5B) are horizontal; that is, on each slice the shear forces on each side of the slice are equal and opposite, so they cancel-when forces are summed in the vertical direction. In general this is not true, so in general the factor of safety will be in error.

Whitman has compared factors of safety computed with the modified Bishop method with those computed with an accurate method. He indicates that, in general, the error is less than 7% and commonly is less than 2%. He indicates that more serious errors can develop if the factor of safety is less than one.

You should now complete exercise 5 (p. 42). This exercise only has a few slices, but it will give you a better understanding of how the procedure works.

3.4 Janbu and Morgenstern-Price methods of stability analysis

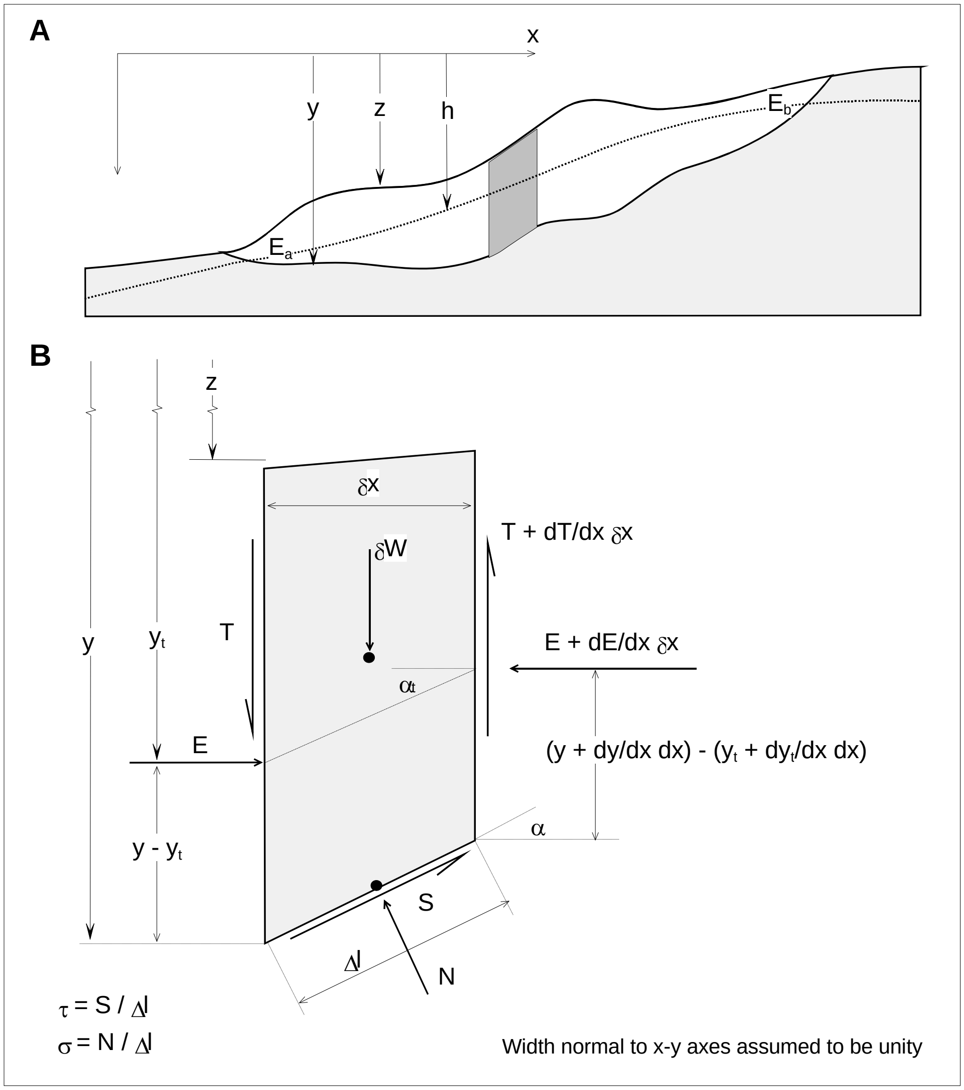

Figure 6. Definition diagram for Janbu and Morgenstern-Price methods of stability.

Janbu (1973) and Morgenstern & Price (1965) have developed similar methods of stability analysis based on a method of slices that are more accurate than the Fellenius or the modified-Bishop methods. They are more accurate because the forces between slices are specifically incorporated in the differential equations. The only significant difference between the Janbu and the Morgenstern-Price methods are the special assumptions introduced in order to make the equilibrium equations determinate. The Morgenstern-Price method assumes a relation between normal and shear forces acting on the sides of the slices. Thus, using the notation shown in Figure 6, they assume,

$$T = \lambda\, f(x)\, E \tag{3.4.1}$$

in which λ is a constant and, in general,

$$f(x) = k\, x + m \tag{3.4.2}$$

in which k and m are constants. We will not follow the derivation presented by Morgenstern-Price (1965) rather we will use Janbu's method of solution.

In the Janbu analysis, one assumes the height of thrust, E, above the base of the side of a slice. One selects a value of η (*eta*), which is the ratio between the height of thrust and the total height of the side of the slice. For *passive* conditions, where the soil is being compressed, η should be somewhat greater than 0.33, and for *active* conditions, where the soil is being extended, η should be somewhat less than 0.33. In general we first work a problem with η of 0.33 everywhere, and then adjust η for the sides of each slice according to whether active or passive conditions occur there. What is the logic of choosing 0.33?[8]

The coordinate system is shown in Figure 6. This same coordinate system is used for the Morgenstern-Price and the Janbu analyses (and in our computer program), but it is different from that presented by Janbu. It is important that you use the coordinate system shown in Figure 6 when you use our computer program or Excel workbook; otherwise, you will get nonsense. Note that positions of surfaces are measured with positive distances *downward* from your reference, x-axis. You use negative distances if the point is above your reference, x-axis. For the problem shown in Figure 6, all the vertical distances are positive.

As in our exact analyses of stability of an infinite slope, we satisfy conditions of moment and force equilibrium. Referring to Figure 6, summation of moments requires that $[\sum M = 0]$ (about the center of the slice at it's base);

$$T\frac{\delta x}{2} + \left[T + \frac{dT}{dx}\delta x\right]\frac{\delta x}{2} + [E + \frac{dE}{dx}\,\delta x]\,[y + \frac{dy}{dx}\frac{\delta x}{2} - y_t + \frac{dy_t}{dx}\,\delta x] - E\,[y + \frac{dy}{dx}\frac{\delta x}{2} - y_t] = 0 \tag{3.4.3}$$

where E is the lateral force acting on a slice

Here y_t is the position of the thrust. Rearranging and dividing by δx, and eliminating the second term in eq. (3.4.3) because it contains the negligible quantity δx^2

$$T = E\tan(\alpha_t) - \frac{dE}{dx}\,(y - y_t); \tag{3.4.4}$$

$$\frac{dy_t}{dx} = -\tan(\alpha_t) \tag{3.4.5}$$

In the Janbu analysis we define η such that

$$(y - y_t) = (y - z)\,\eta \tag{3.4.6}$$

so that

$$\boxed{T = E\tan(\alpha_t) - \frac{dE}{dx}\,(y - z)\,\eta} \tag{3.4.7}$$

This is one of the basic equations.

Summing vertical forces, $[\sum F_y = 0]$;

[8] See Lambe & Whitman (1969, p. 167-168).

$$dW - \frac{dT}{dx}\ \delta x - N\cos(\alpha) - S\sin(\alpha) = 0 \tag{3.4.8}$$

Using the identities,

$$N = \frac{\sigma\ \delta x}{\cos(\alpha)} \tag{3.4.9a}$$

$$S = \frac{\tau\ \delta x}{\cos(\alpha)}\ , \tag{3.4.9b}$$

$$\sigma = \frac{dW}{dx} - \frac{dT}{dx}\ - \tau\tan(\alpha) \tag{3.4.10}$$

We will use eq. (3.4.10) to eliminate σ in other equations.

Summing forces in the *x*-direction, $[\sum F_x = 0]$;

$$E - [E + \frac{dE}{dx}\ \delta x] + S\cos(\alpha) - N\sin(\alpha) = 0 \tag{3.4.11a}$$

Eliminating *S* and *N* with eqs. (3.4.9),

$$\frac{dE}{dx}\ = \tau - \sigma\tan(\alpha) \tag{3.4.11b}$$

Using eq. (3.4.10),

$$\boxed{\frac{dE}{dx} = \tau\{1 + \tan^2(\alpha)\} - \left[\frac{dW}{dx} - \frac{dT}{dx}\right]\tan(\alpha)} \tag{3.4.12}$$

Equation (3.4.12) will be another basic equation.

Now let us compute the factor of safety. We imagine integrating eq. (3.4.12) over the entire length of the slide block. The thrust at the left-hand end is E_a and that at the right-hand end is E_b Both of these may be zero, or E_a may be the thrust against a retaining wall. Thus, integrating eq. (3.4.12),

$$E_b - E_a = \int_a^b \tau\{1 + \tan^2(\alpha)\} - \left[\frac{dW}{dx} - \frac{dT}{dx}\right]\ \tan(\alpha)\ dx \tag{3.4.13}$$

At this point we introduce the shear strength of the soil, that is, the shear stress at failure,

$$\tau_f = \overline{C} + (\sigma - u)\tan(\overline{\phi}) \tag{3.4.14}$$

The shear stress along the sliding surface is assumed to be so the fraction of the failure strength of the soil,

$$\tau = \frac{\tau_f}{F} \tag{3.4.15}$$

where *F* is the factor of safety.

Substituting eq. (3.4.15) into (3.4.13), and solving for *F*,

$$F = \frac{\int_a^b \tau\{1 + \tan^2(\alpha)\}\, dx}{E_b - E_a + \int_a^b \left[\frac{dW}{dx} - \frac{dT}{dx}\right] \tan(\alpha)\, dx} \qquad (3.4.16)$$

This is the same as eq. 90 in Janbu (1973, p 66). Finally, substituting eq. (3.4.15) into eq. (3.4.10) and the resulting (3.4.10) into (3.4.14), we derive,

$$\tau_f = \frac{\bar{C} + \left[\frac{dW}{dx} - \frac{dT}{dx} - u\right] \tan(\bar{\phi})}{1 + \frac{\tan(\alpha)\tan(\bar{\phi})}{F}} \qquad (3.4.17)$$

This is the same as equation 91 in Janbu (1973, p. 66). Equations (3.4.16) and (3.4.17) are to be solved iteratively in order to compute the factor of safety against sliding. The other equations we need in deriving the solution are eqs. (3.4.7), and (3.4.12) and (3.4.15). Combining equations (3.4.12) and (3.4.15) we get

$$\frac{dE}{dx} = \frac{\tau_f}{F} [1 + \tan^2(\alpha)] - \left[\frac{dW}{dx} - \frac{dT}{dx}\right] \tan(\alpha) \qquad (3.4.18a)$$

and here we simply repeat equation (3.4.7, or eq. 88 in Janbu (1973, p. 65))

$$T = E \tan(\alpha_t) - \frac{dE}{dx} (y - z)\, \eta \qquad (3.4.18b)$$

The following quantities are known:	E_b, E_a, $\bar{C}$, $\bar{\phi}$
For each slice we know:	dW, dx, u, α, η, y, z
The following quantities are to be determined:	F, T, E, τ_f

We have the complete set of equations that must be solved in order to compute the factor of safety against sliding. The computer quickly solves the equations. The method of solution can be illustrated by considering two iterations:

1st iteration: For the first iteration we assume that $dT/dx = 0$. In this case it is clear that eqs. (3.4.16) and (3.4.17) can be solved iteratively to determine the first estimate of the factor of safety. In order to prepare for the second iteration, we solve eq. (3.4.18a), with $dT/dx = 0$. Then we solve eq. (3.4.18b) for *T*. Now we are ready for the second iteration.

2nd iteration: For the second and higher iterations, we use the values of *T* and *E* computed during the previous iteration to once more solve eqs. (3.4.16) and (3.4.17) iteratively for the factor of safety. Then we solve eq. (3.4.18a), iterations but this time we use values of *dt/dx* computed during the previous iteration. Then we again solve eq. (3.4.18b) for *T*.

This iterative process is repeated until the factor of safety no longer changes appreciably.

Thus far we have used the value of η of 0.33 for the computation scheme. The next step is to examine values of thrust, *E*, and determine where active and passive zones exist, and adjust values of η accordingly. We can specify a different value of η for each boundary between slices. At the same time we examine the values of thrust to determine where *E* is tensile. If we judge that the soil cannot withstand tension, we insert a tension crack in the slide block at the appropriate place and redo the computations. If the crack is filled with water, the force the water exerts on the soil should be added as a thrust, E_b.

Our computer program (or Excel workbook) prints out values of stresses on the sides and bottom of each element that you have selected for the analysis of a landslide. By studying these stresses, as well as Janbu's paper, you can learn quite a bit more about the stability problem that I have mentioned above. If you are going to do stability analyses of real landslides, you should become quite familiar with Janbu's paper and use the results the computer gives you in order to make fine adjustments in estimates of η as well as of the shape of potential slide surfaces. The method is very powerful and therefore warrants some considerable effort on your part. You can, of course, program the analysis for any computer, perhaps even a programmable calculator.

Now redo exercise 5 using a Janbu analysis. You should use either of the attached programs (BASIC or C/C++) or the supplied Excel spreadsheet. It is important that you use the correct coordinate system!

4. References

Alphabetical listing of references

Abramson, L. W., Lee, T. S., Sharma, S. & Boyce, G. M. 1996. *Slope stability and stabilization methods*. John Wiley & Sons, New York.

Allen, J. R. L. 1969. The maximum slope-angle attainable by surfaces underlayn by bulked equal spheroids with variable dimensional ordering. *Geological Society of America Bulletin* **80**(10), 1923-1930.

Allen, J. R. L. 1970a. The angle of initial yield of haphazard assemblages of equal spheres in bulk. *Geologie en Mijnbouw* **49**(1), 13-22.

Allen, J. R. L. 1970b. The avalanching of granular solids on dune and similar slopes. *Journal of Geology* **78**, 326-351.

Anderson, S. A. & Sitar, N. 1995. Shear strength and slope stability in a shallow clayey soil regolith. In: *Clay and shale slope instability* (edited by Haneberg, W. C. & Anderson, S. A.). *Reviews in Engineering Geology* **X**. Geological Society of America, Boulder, Colorado, 1-12.

Bauer, A. & Calder, P. N. 1971. The influence and evaluation of blasting on stability. In: *Stability in open pit mining* (edited by Brawner & Milligan). Society of Mining Engineers, American Institute of Mechanical Engineers, New York, NY, 83-94.

Baum, R., Fleming, R. W. & Ellen, S. 1989. *Maps showing landslide features and related ground deformation in the Woodlawn area of the Manoa Valley, City and County of Honolulu, Hawaii.* United States Geological Survey Open-File Report **89-290**, 16 p.

Baum, R. L. & Fleming, R. W. 1989. *Landslides and debris flows in Ephraim Canyon, central Utah.* United States Geological Survey Bulletin **1842-C**, 12 p.

Baum, R. L. & Fleming, R. W. 1991. Use of longitudinal strain in identifying driving and resisting elements of landslides. *Geological Society of America Bulletin* **103**(8), 1121-1132.

Baum, R. L., Fleming, R. W. & Johnson, A. M. 1993. *Kinematics of the Apsen Grove landslide, Ephraim Canyon, central Utah.* United States Geological Survey Bulletin **1842F**, 34 p.

Baum, R. L. & Johnson, A. M. 1993. *Steady movement of landslides in fine-grained soils - a model for sliding over an irregular slip surface.* United States Geological Survey Bulletin **1842**, D1-D28 p.

Baum, R. L., Johnson, A. M. & Fleming, R. W. 1988. *Measurement of slope deformation using quadrilaterals.* United States Geological Survey Bulletin **1842-B**, 23 p.

Baum, R. L. & Reid, M. E. 1995. Geology, hydrology, and mechanics of a slow-moving, clay-rich landslide, Honolulu, Hawaii. In: *Clay and shale slope instability* (edited by Haneberg, W. C. & Anderson, S. A.). *Reviews in Engineering Geology* **X**. Geological Society of America, Boulder, Colorado, 79-106.

Bishop, A. W. 1955. The use of the slip circle in the stability analysis of slopes. *Géotechnique* **5**, 7-17.

Bromhead, E. N. 1978. Large landslides in London Clay at Herne Bay, Kent. *Quarterly Journal of Engineering Geology* **11**, 291-304.

Cabrera, J. G. 1976. Factors relating to landslide process in Canadian quickclays. *Earth Surface Processes* **1**, 163-172.

Cabrera, J. G. & Smalley, I. J. 1973. Quickclays as products of glacial action: A new approach to their nature, geology, distribution and geotechnical properties. *Engineering Geology* **7**, 115-133. .

Caldenius, C. & Lundström, R. 1966. *The landslide at Surte on the river Göta Älv*. Sveriges Geologiska Undersökning.

Casagrande, A. 1975. Liquifaction and cyclic deformation of sands, A critical review. *Proceedings of the 5th Pan Americal Conference on Soil Mechanics and Foundation Engineering* **5**, 79-133.

Chen, R. H. & Chameau, J.-L. 1982. Three-dimensional limit equilibrium analysis of slopes. *Géotechnique* **32**, 31-40.

Cook, J. L. 1991. *Conversion factors*. Oxford University Press, Oxford.

Cornforth, D. H. & Mikkelsen, P. E. 1996. Continuous monitoring of the slope above an excavation within a marginally stable landslide. In: *Seventh International Symposium on Landslides* (edited by Senneset, K.) **3**. A.A. Balkema, Trondheim, Norway, 1539-1544.

Crandell, D. R. & Varnes, D. J. 1961. *Movement of the Slumgullion earthflow near Lake City, Colorado.* United States Geological Survey Professional Paper **P 0424-B**, B136-B139 p.

Crawford, C. B. & Eden, W. J. 1967. Stability of natural slopes in sensitive clay. *Journal of the Soil Mechanics and Foundations Division, Proceedings of the American Society of Civil Engineers* **93**(SM 4), 419-436.

Fetter, C. W. 1994. *Applied hydrogeology*. Prentice-Hall, New York.

Fleming, R. W., Ellen, S. D. & Algus, M. A. 1989. Transformation of dilative and contractive landslide debris into debris-flow - an example from Marin County, California. *Engineering Geology* **27**, 201-223.

Fleming, R. W. & Johnson, A. M. 1975. Rates of seasonal creep of silty clay soil. *Quarterly Journal of Engineering Geology* **8**, 1-29.

Fleming, R. W. & Johnson, A. M. 1989. Structures associated with strike-slip faults that bound landslide elements. *Engineering Geology* **27**, 39-114.

Fleming, R. W. & Johnson, A. M. 1994. *Landslides in colluvium.* United States Geological Survey Bulletin **2059-B**, 24 p.

Fleming, R. W., Johnson, A. M., Hough, J. E., Gocke, A. O. & Lion, T. 1981. Engineering geology of the Cincinnati area. In: *Geological Society of America Annual Meeting Field Trip Guidebook* **Field Trip No. 18**. Geological Society of America, Boulder, CO, 543-570.

Fleming, R. W., Johnson, R. B. & Schuster, R. L. 1988a. The reactivation of the Manti landslide, Utah. In: *The Manti, Utah, landslide* **1311**. United States Geological Survey Professional Paper, Washington, D.C., 1-22.

Fleming, R. W., Johnson, R. B., Schuster, R. L. & Williams, G. P. 1988b. *The Manti, Utah, landslide.* United States Geological Survey Professional Paper **1311**, 69 p.

Freeze, R. A. & Cherry, J. A. 1979. *Groundwater*. Prentice-Hall, Inc., Englewood Cliffs, New Jersey.

Hall, D. E., Long, M. T. & Remboldt, M. D. 1994. Slope stability reference guide for National Forests in the United States **EM-7170-13**. United States Department of Agriculture, Forest Service, Washington, D.C., 1091.

Haneberg, W. C. 1991a. Observation and analysis of pore pressure fluctuations in a thin colluvium landslide complex near Cincinnati, Ohio. *Engineering Geology* **31**, 159-184.

Haneberg, W. C. 1991b. Pore pressure diffusion and the hydrologic response of nearly saturated, thin landslide deposits to rainfall. *Journal of Geology* **99**, 886-892.

Haneberg, W. C. 1995. Groundwater flow and the stability of heterogeneous infinite slopes underlayn by impervious substrata. In: *Clay and shale slope instability* (edited by Haneberg, W. C. & Anderson, S. A.). *Reviews in Engineering Geology* **X**. Geological Society of America, Boulder, Colorado, 63-78.

Haneberg, W. C. & Anderson, S. A. 1995. Clay and shale slope instability. In: *Reviews in Engineering Geology* **X**. Geological Society of America, Boulder, Colorado.

Haneberg, W. C. & Gökce, A. Ö. 1994. *Rapid water-level fluctuations in a thin colluvium landslide west of Cincinnati, Ohio.* United States Geological Survey Bulletin **B 2059-C**, C16 p.

Haneberg, W. C. & Tripp, G. 1991. An irrigation-induced debris flow in northern New Mexico. *Bulletin of the Association of Engineering Geologists* **28**(4), 359-374.

Hansen, W. R. 1965. Effects of the earthquake of March 27 1964, at Anchorage, Alaska. *United States Geological Survey Professional Paper* **542**, 30-66.

Harp, E. L., Wells, W. G., II & Sarmiento, J. G. 1990. Pore pressure response during failure in soils. *Geological Society of America Bulletin* **102**(4), 428-438.

Hoexter, D. F., Holzhausen, G. & Soto, A. E. 1987. A method of evaluating the relative stability of ground for hillside development. *Engineering Geology* **12**, 319-336.

Hutchinson, J. N. 1986. A sliding-consolidation model for flow slides. *Canadian Geotechnical Journal* **23**, 115-126.

Iverson, R. M. 1983. A model for creeping flow in landslides. *Bulletin of the Association of Engineering Geologists* **20**, 455-459.

Iverson, R. M. 1985. A constitutive equation for mass movement behavior. *Journal of Geology* **93**(2), 143-160.

Iverson, R. M. 1986a. Dynamics of slow landslides: a theory for time-dependant behavior. In: *Hillslope Process* (edited by Abrahams, A. D.). Allen and Unwin, Boston, 287-317.

Iverson, R. M. 1986b. Unsteady, nonuniform landslide motion: 1. Theoretical dynamics and the steady datum state. *Journal of Geology* **94**, 1-15.

Iverson, R. M. 1986c. Unsteady, nonuniform landslide motion: 2. Linearized theory and the kinematics of transient response. *Journal of Geology* **94**, 349-364.

Iverson, R. M. 1990. Groundwater flow fields in infinite slopes. *Géotechnique* **40**(1), 139-143.

Iverson, R. M. 1993. Differential equations governing slip-induced pore-pressure fluctuations in a water-saturated granular medium. *Mathmatical Geology* **25**(8), 1027-1048.

Iverson, R. M. & LaHusen, R. G. 1989. Dynamic pore-pressure fluctuations in rapidly shearing granular materials. *Science* **246**, 796-799.

Iverson, R. M. & Major, J. J. 1986. Groundwater seepage vectors and the potential for hillslope failure and debris flow mobilization. *Water Resources Research* **22**(11), 1543-1548.

Iverson, R. M. & Major, J. J. 1987. Rainfall, ground-water flow, and seasonal movement at Minor Creek landslide, northwestern California: Physical interpretation of empirical relations. *Geological Socisty of America Bulletin* **99**(10), 579-594.

Iverson, R. M. & Reid, M. E. 1992. Gravity-driven groundwater flow and slope failure potential 1. Elastic effective-stress model. *Water Resources Research* **28**(3), 925-938.

Jacobson, B. 1952. *The landslide at Surte on the Gota river*. Royal Swedish Geotechnical Institute Proceedings.

Jäger, S. & Wieczorek, G. F. 1994. *Landslide susceptibility in the Tully Valley area, Finger Lakes region, New York.* United States Geological Survey Open File Report **OF-94-615**, p.

Janbu, N. 1973. Slope stability computations. In: *Embankment-Dam engineering* (edited by Hirschfeld, R. C. & Poulos, S. J.) **Casagrande**. John Wiley & Sons, New York, 47-86.

Johnson, A. M. 1965. A model for debris flow. Unpublished Ph.D. thesis, Pennsylvania State University, University Park, PA.

Johnson, A. M. 1970. *Physical processes in geology*. Freeman, Cooper & Company, San Francisco.

Johnson, A. M. 1984. Debris flow. In: *Slope Instability* (edited by Brunsden, D. & Prior, D. B.). John Wiley and Sons, London, 257-361.

Johnson, A. M. 1996. *A model for grain flow and debris flow.* United States Geological Survey Open-File Report **96-726**, 41 p.

Johnson, A. M. & Baum, R. L. 1987. *BASIC programs for computing displacement, strains, and tilts from quadilateral measurements.* United States Geological Survey Open-file report **87-343**, 19 p.

Johnson, A. M. & Hampton, M. A. 1969. *Subaerial and subaqueous flow of slurries.* United States Geological Survey Final Report **14-08-001-10884**, p.

Johnson, A. M. & Martosudarmo, S. Y. 1997. Discrimination between inertial and macro-viscous flows of fine-grained debris with a rolling-sleve viscometer. In: *1st International conference on debris-flow hazards mitigation: Mechanics, prediction and assessment*, San Francisco, California.

Johnson, S. E. 1997. 1996 Tumalt debris flow and debris avalanches in Columbia River Gorge east of Portland, Oregon. In: *1st International conference on debris-flow hazards mitigation: Mechanics, prediction and assessment*, San Francisco, California.

Kamb, B. 1970. Sliding motion of glaciers: Theory and observation. *Reviews in Geophysics and Space Physics* **8**, 673-728.

Keefer, D. K. 1984. Landslides caused by earthquakes. *Geological Society of America Bulletin* **95**(4), 406-421.

Keefer, D. K. & Johnson, A. M. 1983. *Earth flows: morphology, mobilization and movement.* United States Geological Survey Professional Paper **1264**, 56 p.

Lambe, T. W. & Whitman, R. V. 1969. *Soil mechanics*. John Wiley & Sons, New York, NY.

Lawrence, D. E., Aylsworth, J. M. & Morey, C. R. 1996. Sensitive clay flows along the South Nation Rive, Ontario, Canada and their impact on land use. In: *Seventh International Symposium on Landslides* (edited by Senneset, K.) **1**. A.A. Balkema, Trondheim, Norway, 479-484.

Malvern, L. E. 1969. *Introduction to the mechanics of continuous medium*. Prentice-Hall, Inc., Englewood Cliffs, New Jersey.

Michalowski, R. L. 1995. Stability of slopes: Limit analysis approach. In: *Clay and shale slope instability* (edited by Haneberg, W. C. & Anderson, S. A.). *Reviews in Engineering Geology* **X**. Geological Society of America, Boulder, Colorado, 51-62.

Morgenstern, N. R. & Price, V. E. 1965. The analysis of the stability of general slip surfaces. *Géotechnique* **15**, 79-92.

Noble, H. L. 1973. Residual strength and landslides in clay and shale. *Journal of Soil Mechanics and Foundations, Proceedings of the American Society of Civil Engineers*(SM 9), 705-719.

Palmer, A. C. & Rice, J. R. 1973. The growth of slip surfaces in the progressive failure of over-consolidated clay. *Proceedings of the Royal Society of London* **332**, 527-548.

Reid, M. E. 1994. A pore-pressure diffusion model for estimating landslide-inducing rainfall. *Journal of Geology* **102**, 709-771.

Reid, M. E. & Iverson, R. M. 1992. Gravity-driven groundwater flow and slope failure potential 2. Effects of slope morphology, material properties, and hydraulic heterogeneity. *Water Resources Research* **28**(3), 939-950.

Riestenberg, M. M. 1981. The effect of woody vegetation on stabilizing slopes in the Cincinnati area, Ohio. In: *Biology Department, University of Cincinnati*, 79.

Riestenberg, M. M. & Sovonick-Dunford, S. 1983. The role of woody vegetation in stabilizing slopes in the Cincinnati area, Ohio. *Geological Scoiety of America Bulletin*, 506-518.

Seed, H. B. 1967. Slope stability during earthquakes. *Journal of the Soil Mechanics and Foundations Division, Proceedings of the American Society of Civil Engineers* **93**(SM 4), 299-323.

Seed, H. B. & Wilson, S. D. 1967. The Turnagain Heights Landslide, Anchorage, Alaska. *Journal of the Soil Mechanics and Foundations Division, Proceedings of the American Society of Civil Engineers* **93**(SM 4), 325-353.

Skempton, A. W. 1964. Long term stability of clay slopes. The 1964 Rankine lecture. *Géotechnique* **14**(2), 77-102.

Skempton, A. W. 1966. Some observations on tectonic shear zones. In: *First International Congress on Rock Mechanics*. *Proceedings* **1**, 329-335.

Skempton, A. W. 1985. Residual strength of clays in landslides, folded strata and the laboratory. *Géotechnique* **35**(1), 3-18.

Skempton, A. W. & Pelty, D. J. 1966. The strength along structural discontinuities in stiff clays. *Proceedings, Geotechnical Conference, Oslo* **2**, 29-46.

Torrance, J. K. 1983. Towards a general model of quick clay development. *Sedimentology* **30**, 547-555.

Turner, A. K. & Schuster, R. L. 1996. Landslides: Investigation and mitigation. In: *Special Report* **247**. National Academy Press, Washington, D.C., 675.

Varnes, D. J. 1074. *The logic of geological maps, with reference to their interpretation and use for engineering purposes.* United States Geological Survey Professional Paper **837**, 48 p.

Varnes, D. J. 1962. Analysis of plastic deformation according to Von Mises' Theory with applications to the South Silverton Area, San Juan County Colorado. *Geological Survey Professional Paper* **378-B**, B1-B49.

Varnes, D. J. 1982. Time-deformation relations in creep to failure of earth materials. In: *Proceedings 7th SE Asia Geotechnical Conf., Hong Kong*, 107-130.

Voight, B. 1973. The mechanics of retrogressive block-gliding, with emphasis on the evolution of the Turnagain Heights landslide, Anchorage, Alaska. In: *Gravity and Tectonics* (edited by DeJong, K. & Scholten, R.). John Wiley & Sons, Inc., New York, NY, 97-121.

Voight, B., Janda, R. J., Glicken, H. & Douglass, P. M. 1983. Nature and mechanics of the Mount St. Helens rockslide-avalanche of 18 May 1980. *Géotechnique* **33**, 243-273.

Vonder Linden, K. 1972. An analysis of the Portuguese bend landslide, Palos Verdes Hills, California. In: *Department of Geology, Stanford University*.

Vonder Linden, k. 1989. The Portugese bend landslide. *Engineering Geology* **27**, 301-373.

Waldron, L. J. 1977. The shear resistance of root-permeated homogeneous and stratified soil. *Soil Science Society of America Journal* **41**, 843-849.

Watry, S. M. & Ehlig, P. L. 1995. Effect of test method and procedure on measurements of residual shear strength from Bentonite from the Portuguese Bend landslide. In: *Clay and* *shale slope instability* (edited by Haneberg, W. C. & Anderson, S. A.). *Reviews in Engineering Geology* **X**. Geological Society of America, Boulder, Colorado, 13-38.

Whitman, R. V. & Bailey, W. A. 1967. Use of computers for slope stability analysis. *Journal of the Soil Mechanics and Foundations Division, Proceedings of the American Society of Civil Engineers* **93**(SM-4), 475-497.

Wieczorek, G. F., Gori, P. L., Jäer, S., Kappel, W. M. & Negussey, D. 1996. Assessment and mandagement of landslide hazards near the Tully Valleu landslide, Syracuse, New York, USA. In: *Seventh International Symposium on Landslides* (edited by Senneset, K.) **1**. A.A. Balkema, Trondheim, Norway, 411-416.

Wu, T. H., McKinnell, W. P., III & Swanston, D. N. 1979. Strength of tree roots in a landslide on Prince of Wales Island, Alaska. *Canadian Geotechnical Journal* **16**, 91-33.

Wu, T. H. & Swanston, D. N. 1989. Risk of landslides in shallow soils and its relation to clearcutting in southeastern Alaska. *Forest Science* **26**, 495-510.

References by topic

In this section some papers are grouped by subject. Each subject can make a small reading project in itself. Only the author and date for references are listed in this section. The full references are given in the above section.

Concept of residual and peak strengths

(Skempton 1964)

(Skempton 1985).

Portuguese Bend Landslide, Los Angeles County

(Watry & Ehlig 1995)

(Vonder Linden 1989)

Landslides in colluvium and in lakes clays in the Cincinnati area

(Riestenberg & Sovonick-Dunford 1983)

(Haneberg 1991a)

(Haneberg 1991b)

(Fleming & Johnson 1994)

(Fleming et al. 1981)

(Haneberg & Gökce 1994)

Turnagain Heights Landslide, Alaska

(Hansen 1965)

(Voight 1973)

(Seed & Wilson 1967)

Landslides in sensitive clays and clayshales

(Noble 1973)

(Crawford & Eden 1967)

Clough *et al.* (1977)

Bromhead (1978).

(Lawrence et al. 1996)

Quick clay slides

(Cabrera 1976)

(Cabrera & Smalley 1973)

(Jäger & Wieczorek 1994)

(Torrance 1983)

(Wieczorek et al. 1996)

Landslides in Utah

(Baum & Fleming 1989)

(Baum et al. 1993)

Strain in Landslides

(Baum et al. 1988)

Mapping

(Hoexter et al. 1987)

Landslides in Oregon

Landslides in Portland

(Cornforth & Mikkelsen 1996)

Appendix A. Mohr's Circle

Here we will consider stress boundary conditions and how these can be represented by the Mohr circle. Mohr's circle has found extensive used in mechanics, and is commonly encountered in structural geology, rock mechanics and engineering geology. Mohr's circle provides a graphical way of relating stresses on arbitrarily-oriented surfaces to the principle stresses. It is also used in defining parameters such as cohesion and angle of internal friction.

In order to see where Mohr's circle comes from, below we pose two questions and proceed to answer them. The first question (Figure 7) we will pose is *given a surface inclined at an angle* θ *to two known perpendicular stresses what is the magnitude of the stresses parallel to, and normal to this surface*?

The second question (Figure 8) is *given a surface inclined at an angle* θ *to the principle stress directions, what is the magnitude of the stresses parallel to, and normal to this surface*? As you can see the questions are very similar. The key in the second question is that we are using principle stress directions, so that the planes to which our surface is inclined have no shear stresses acting on them. In the first question there are shear stresses acting on all of the planes. The answer to the second question will lead us to the equations that when graphed give Mohr's circle. We will then see how to use the Mohr's circle to graphically solve the equations we derive. Problem 1 is a more general problem.

The equations we will derive will also allow us to calculate the orientation and magnitude of principle stresses given the stress state on two arbitrarily oriented surfaces. Thus we can get a lot of mileage from the following derivation. After completing the derivation we will go on to explore the properties of the Mohr circle.

Stresses on an inclined plane

Given a surface inclined at an angle θ to two known perpendicular stresses what is the magnitude of the stresses parallel to, and normal to this surface?

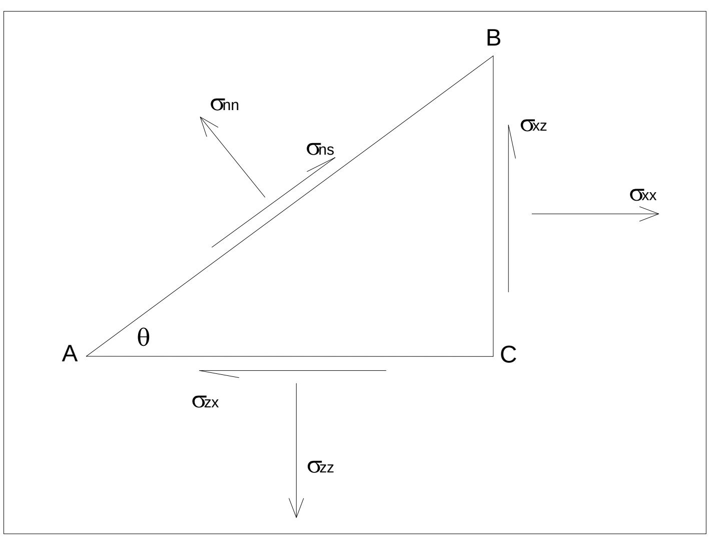

Figure 7. Definition diagram for (a) forces and (b) stresses. σ_{nn} is normal to some inclined plane, σ_{ns} are parallel to the inclined plane.

It is assumed that the element shown in Figure 7 is in equilibrium — that is, it is not accelerating — so all forces will sum to zero. Using force equilibrium we will be able to derive relationships between all the forces in the problem. This is a very routine and standard procedure in mechanics. Almost all equations in mechanics start with summing forces (see for example, Johnson 1970, Malvern 1969).

To sum forces me must convert stresses (Force/Area) to forces by multiplying each stress by the area over which it is acting. We will use "depth" of the surface normal to the page of 1 unit.

From Figure 7 we see that σ_{nn} is acting in the positive x-direction, and it is acting over an area of $A \cdot B \cdot 1$ (where 1 is the unit depth). Thus the force in the *n*-direction is simply

$$\sigma_{nn} AB. \tag{A.1.1}$$

Now we consider the σ_{xx} stress. It is acting over an area of $B \cdot C \cdot 1$. Thus the force acting on this surface is

$$\sigma_{xx} BC \tag{A.1.2}$$

The force is acting at an angle θ to the *n*-direction, so only part of this force is acting in the *n*-direction. Using vector algebra we see that the component of the force acting in the *n*-direction is

$$-\sigma_{xx} BC \sin(\theta) \tag{A.1.3}$$

since the force is acting in the **negative** *n*-direction.

Proceeding as above for each of the stresses in Figure 7. Summing forces in the direction normal to the inclined surface (the *n*-direction) gives

$$\sigma_{nn} AB + \sigma_{xz} BC \cos(\theta) + \sigma_{xz} AC \sin(\theta) - \sigma_{xx} BC \sin(\theta) - \sigma_{zz} AC \cos(\theta) = 0 \tag{A.1.4}$$

Dividing through by *AB* and recognizing that[9]

$$\sin(\theta) = \frac{BC}{AB} \tag{A.1.5a}$$

$$\cos(\theta) = \frac{AC}{AB} \tag{A.1.5b}$$

we get

$$\sigma_{nn} + 2\,\sigma_{xz} \sin(\theta)\cos(\theta) - \sigma_{xx} \sin^2(\theta) - \sigma_{zz} \cos^2(\theta) = 0 \tag{A.1.6}$$

solving for σ_{nn}

$$\sigma_{nn} = \sigma_{xx} \sin^2(\theta) + \sigma_{zz} \cos^2(\theta) - 2\,\sigma_{xz} \sin(\theta)\cos(\theta) \tag{A.1.7}$$

This completes the first step. We have a relationship between the normal stress and the stresses on the other surfaces. Now we continue to find an expression for the shear stress on the inclined surface, σ_{ns}, by summing forces in the *s*-direction

$$\sigma_{ns} AB + \sigma_{zx} BC \sin(\theta) + \sigma_{zx} AC \cos(\theta) + \sigma_{xx} BC \cos(\theta) + \sigma_{zz} AC \sin(\theta) \tag{A.1.8}$$

Again, dividing through by *AB* and substituting in trigonometric identities given above

$$\sigma_{ns} + \sigma_{xz} \sin^2(\theta) + \sigma_{zx} \cos^2(\theta) + \sigma_{xx} \sin(\theta)\cos(\theta) + \sigma_{zz} \sin(\theta)\cos(\theta) = 0 \tag{A.1.9}$$

---

[9] From the equations for a right-triangle: sin(θ) = opposite / hypotenuse ; cos(θ) = adjacent / hypotenuse ; tan(θ) = opposite / adjacent

solving for σ_{ns}

$$\sigma_{ns} = (\sigma_{zz} - \sigma_{xx}) \sin(\theta) \cos(\theta) + \sigma_{xz}(\cos^2(\theta) - \sin^2(\theta)) \quad \text{(A.1.10)}$$

Thus our results are:

$$\sigma_{nn} = \sigma_{xx} \sin^2(\theta) + \sigma_{zz} \cos^2(\theta) - 2\, \sigma_{xz} \sin(\theta) \cos(\theta) \quad \text{(A.1.11a)}$$

$$\sigma_{ns} = (\sigma_{zz} - \sigma_{xx}) \sin(\theta) \cos(\theta) + \sigma_{xz}(\cos^2(\theta) - \sin^2(\theta)) \quad \text{(A.1.11b)}$$

Mohr's Circle

We now consider a slightly more specialized form of the equations that will yield Mohr’s circle. The question posed here is: given a surface inclined at an angle θ to the principle stress directions, what is the magnitude of the stresses parallel to, and normal to this surface?

Figure 8. Definition diagram for the derivation of Mohr’s circle.

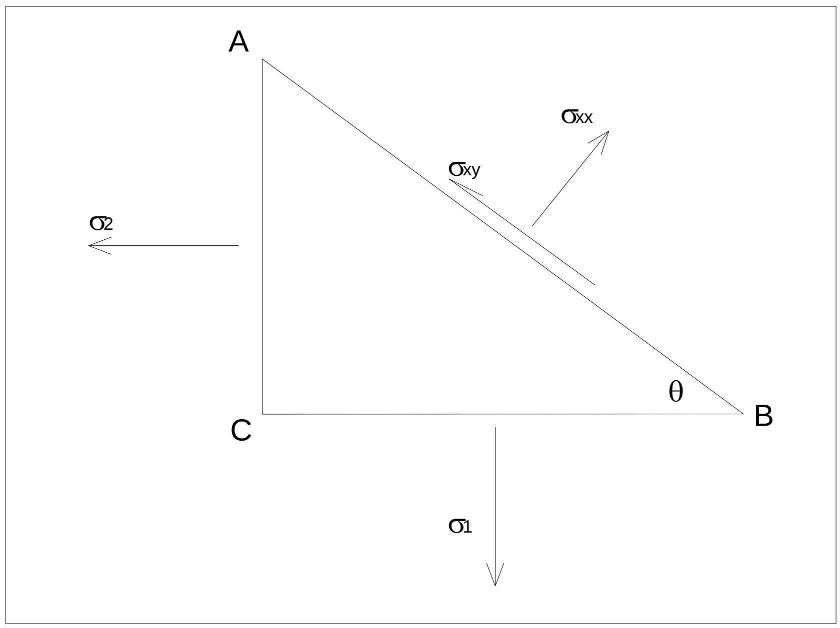

This is a very similar case to that considered above only in this case we know the principal stresses, σ_1 and σ_2, so there are no shear stresses acting on those planes. We have defined a positive *x*- and *y*-coordinate system as shown in Figure 8. We assume that the body is in equilibrium, so we start by summing forces in the *x*-direction

$[\Sigma F_x = 0]$

$$\sigma_{xx}\, AB - \sigma_1\, BC \cos(\theta) - \sigma_2\, AC \sin(\theta) = 0 \quad \text{(A.2.1a)}$$

$$\sigma_{xx} - \sigma_1\, BC/AB \cos(\theta) - \sigma_2\, AC/AB \sin(\theta) = 0 \quad \text{(A.2.1b)}$$

recognizing that

$$BC/AB = \cos(\theta) \text{ and } AC/AB = \sin(\theta) \quad \text{(A.2.2)}$$

We get

$$\sigma_{xx} = \sigma_1 \cos^2(\theta) + \sigma_2 \sin^2(\theta) \quad \text{(A.2.3a)}$$

Now we sum forces in the y-direction. Following the same procedure as above, you can show that you will get (the reader should perform the operations)

$$\sigma_{xy} = \sigma_1 - \sigma_2 (\cos(\theta) \sin(\theta)) \qquad \text{(A.2.3b)}$$

Using the following trigonometric identities

$$\cos^2(\theta) = ½(1+\cos(2\theta)) \qquad \text{(A.2.4a)}$$

$$\sin^2(\theta) = ½ (1- \cos(2\theta)) \qquad \text{(A.2.4b)}$$

$$\sin(\theta)\cos(\theta) = ½ (\sin(2\theta)) \qquad \text{(A.2.4c)}$$

We end up with the following relationships

$$\sigma_{xx} = (\sigma_1 + \sigma_2)/2 + (\sigma_1 - \sigma_2)/2 \cos(2\theta) \qquad \text{(A.2.5a)}$$

$$\sigma_{xy} = (\sigma_1 - \sigma_2) \sin(2\theta) \qquad \text{(A.2.5b)}$$

These equations have the form of a circle. These are the equations for Mohrs circle, they relate the stress on any plane to the orientation of the plane with respect to the principle stresses.

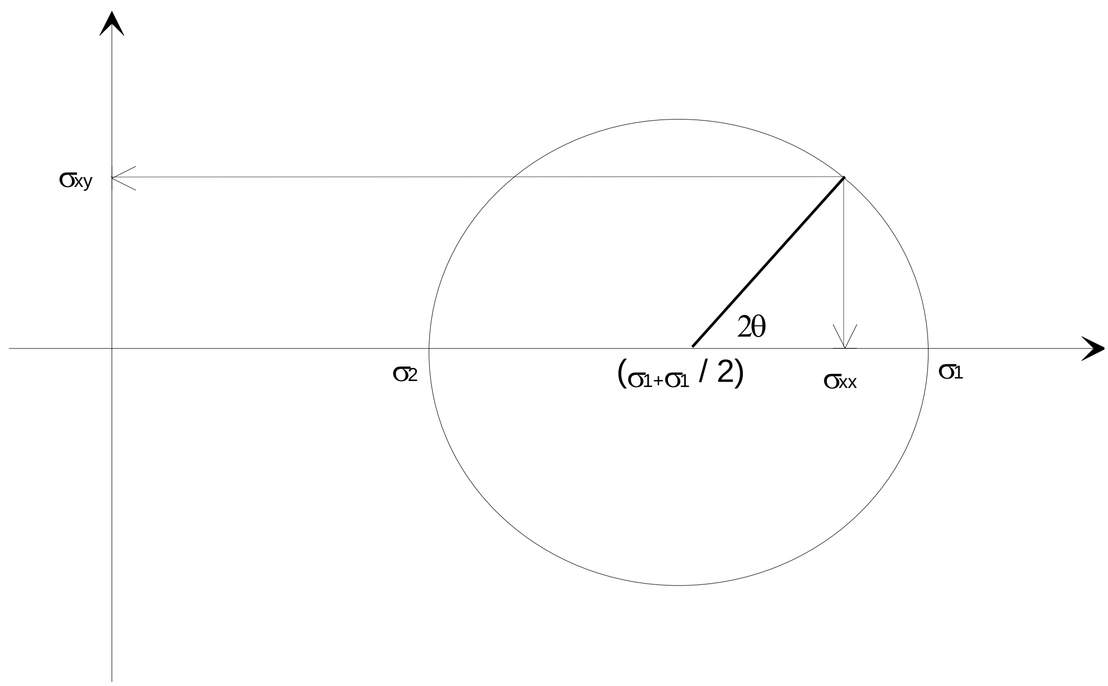

Figure 9. Mohr’s circle showing the parameters in the equations derived above.

Appendix B. Exercises

Exercise 1 – Dry Soil

Assume the following properties for the dry soil:

- Cohesion, C = 4800 Pa
- Internal friction angle, ϕ = 20°
- Unit weight, γ = 20,000 N m^{-3}

I suggest you do all these calculations in a spreadsheet. The spreadsheet will be more useful if you have single cells where you enter values for *C*, ϕ, γ, and later the void ratio, Θ. All calculations should link back to these cells. Changing the values of these cells will cause the spreadsheet to recalculate and re-plot your results allowing you to easily generate plots for different cases. We will be adding to this worksheet as time goes on so try to make the worksheet as general as possible, it will become a useful tool for future calculations, even outside this class.

1. Plot the critical thickness, t_c, as a function of the slope angle, where the slope angle ranges from 0° to 90°. You will also want to construct a second plot showing the range of slope angles where the critical thickness changes rapidly.
2. What general conclusions can you reach from the plots you generated in part 1. For example, you will want to use the critical thickness equation to explain why the curve has this shape. Is this shape limited to this set of numbers, or do all possible curves have this shape? What controls the critical parts of this curve – that is what is the major control on the critical thickness. Part of the curve makes no sense physically, dash that part and explain why it is invalid.
3. Suppose that we expect failure at the soil-rock interface, and that the soil is 3 m thick and the slope angle is 25°. What is the factor of safety against sliding? How does the factor of safety change if you only vary the soil thickness, for example, what is the factor of safety against sliding at half the thickness of the soil?
4. Many landslides in colluvium in Cincinnati are about one meter thick and occur on slopes with slope angles of about 25°. Plot the relation between cohesion (*C*) and angle of internal friction (ϕ) that would provide a factor of safety of one under such conditions. Using a range of internal friction angles (say 5° to 45°), what is the difference in the plots? The maximum value of angle of internal friction that you should use is 25° – why?

Exercise 2 – Standing water

For this exercise we have a submerged slope. Assume that the porosity of the soil is 20% and that the soil is saturated with water (no air in pore spaces). The dry unit weight, the cohesion and the angle of internal friction are assumed to be the same as those given above. In this problem, γ in exercise 1 is γ_t in equation (2.3.15a). In section 2.2 we used γ for simplicity. For landslides we always use total unit weight, γ_t, which is more precisely defined in equations 2.3.15.

1. Plot the critical thickness, t_c, as a function of the slope angle, where the slope angle ranges from 0° to 90°. You will also want to construct a second plot where the slope angle ranges from 0° to about 35°. Plot the relation between critical thickness and slope angle on the same graph as in exercise 1.
2. Suppose that we expect failure at the soil-rock interface, and that the soil is 3 m thick and the slope angle is 25°. What is the factor of safety against sliding? How does the factor of safety change if you only vary the soil thickness, for example, what is the factor of safety against sliding at half the thickness of the soil?
3. Compare the results from part 1 and 2 in this exercise with the results from parts 1 and 3 in Exercise 1.
4. How do you expect the angle of internal friction and cohesion of a dry soil to change when it is saturated? How large is the change in each? How do you think this will affect the results of your calculations?

Exercise 3 – Seepage

Plot a third curve for critical thickness as a function of slope angle on the graph constructed for exercises 1 & 2. Use the same parameters as the previous exercises.

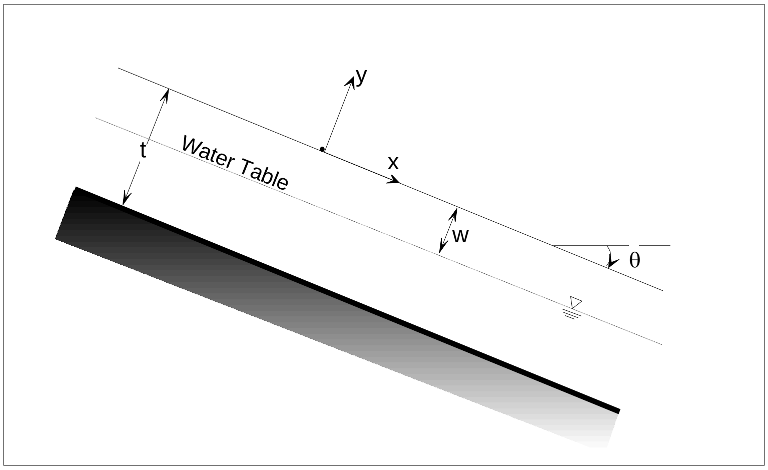

Figure 10. Definition diagram for exercise 3.

Solve the problem analogous to that treated above, but this time for a water table that is a distance *w* (measured normal to the slope) below the ground surface, where $0 < w < t$. Plot curves on the diagram constructed for assignment 1, for values of w/t of 0, 0.25, 0.5, 0.75 and 1.0. Write out the formula that you develop. Show that for $w/t = 1$ the equation becomes the equation for a dry slope, and that for $w/t = 0$ the equation becomes that for seepage parallel to the slope (the equation you used in part 1).

Apply the formula you developed for part 2 to a landslide at McKelvey Road in Cincinnati. Önder Gökce has made a detailed study of the landslide and following are some of the relevant data. The landslide was active at the time the measurements were taken.

- The landslide is about 75 meters long (from head to toe), and about 10 meters deep (measured vertically).
- The average slope of the ground surface is about 8°.
- During drilling of three boreholes through the slide mass it was noted that the soil, which consists of about 7 m of till overlying about 3 m of glacial lake-clay, was rather dry until we had drilled through the lake clay and through one or two limestone beds in the bedrock underlying the lake clay. Then the cuttings became very wet (muddy) and after a few hours water rose in the borehole to a level of 0.5 to 1.5 m from the ground surface (depending on the time of year).

Using these data, you are to compute the residual angle of internal friction of the lake clay involved in the sliding.

Exercise 4 – Tree Roots

Mary Riestenberg determined and estimated the following parameters for a landslide that she studied in Cincinnati:

$\overline{C} = 0$

$\theta = 35°$

$\overline{\phi} = 12°$

$\gamma_w = 9.8$ kN/m^3

$t = 0.5$ m

$\gamma_t = 19.6$ kN/m^3

$$(1/A) \sum_{i=1}^{n} F_i = 5.7 \text{ kN/m}^2$$

You are to determine the factor of safety against sliding.

What is the effect of roots on the slide mass. What is the factor of safety without roots? How do roots enter the factor of safety calculation – what is what soil property do they change – and how would we model their effect. That is, if we were to do a back calculation for material parameters, what property would root strength be indistinguishable from.

Exercise 5 – Fellenius Method

In order to "get the feel" for computation of stability factors, determine the factor of safety against sliding for the slope shown below:

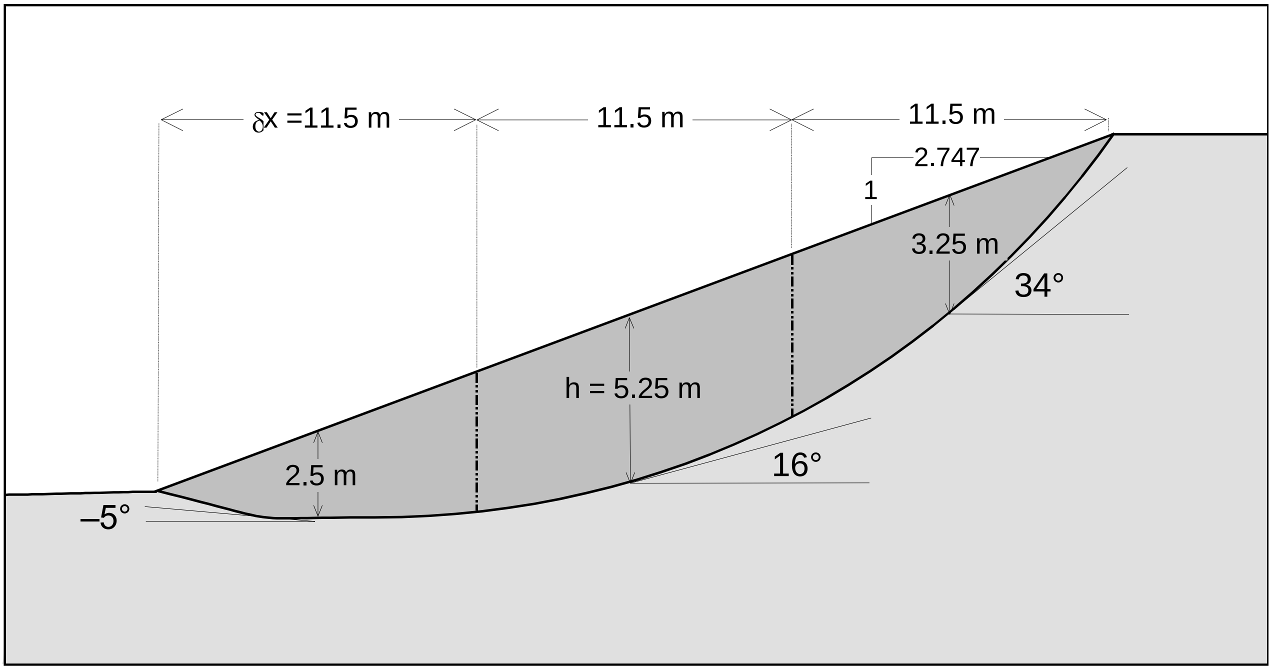

Figure 11. Definition diagram for exercise 5.

The water table is assumed to be at the upper surface of the slide, and, using the solution for pore-water pressures in an infinite slope, we compute

$r_u = (u/\gamma h) \cong 0.37 \cong 0.4$

in which h is the height of the slice (see figure below) and γ is the saturated unit weight of the soil. The parameters are,

- $\bar{C}$ = 16 kN/m^2
- γ = 24 kN/m^3
- $\bar{\phi}$ = 14°

Table 2. Some of the important parameters for each slice in exercise 5.

Slice	δx_i (m)	h_i (m)	W_i (kN)	ϑ_i	u_i (kN/m^2)
1	11.5	2.5	690	–5°	24
2	11.5	5.25	1450	+16	50.4
3	11.5	3.25	900	+34	31.2

For problems other than this one, of course, you would use many more than three slices. The purpose is for you to be able to quickly solve a problem approximately; the method is what is important right now, not the result.

First, compute the factor of safety using the Fellenius method (Answer is approximately F = 1.16). Then, start with an estimated factor of safety of 1.0 and iterate the modified-Bishop solution three times in order to estimate the factor of safety by that method.

As a second exercise, use the Fellenius method to "back calculate" the residual strength of the soil involved in the slide shown in the figure on pg. 43. This is a method that we commonly use in analyzing existing landslides. The residual cohesion, $\overline{C}_r$ is generally nearly zero, so we set it equal to zero. Then we set the factor of safety equal to 1.0 and compute the angle of residual friction, $\overline{\phi}_r$.

It is presumably clear, upon examination of eq. (3.1.6), that we can solve directly for the residual friction,

$$\tan(\overline{\phi}_r) = [\sum W_i \sin(\vartheta_i)] / [\sum \overline{N}_i] \qquad (3.3.6)$$

in which

$$\overline{N}_i = N_i - U_i \text{ and } N_i = W_i \cos(\vartheta_i)$$

for the Fellenius method, and U_i is given by eq. (3.3.2b).

Exercise 6 – Janbu Method

PART I

Given the following landslide geometry:

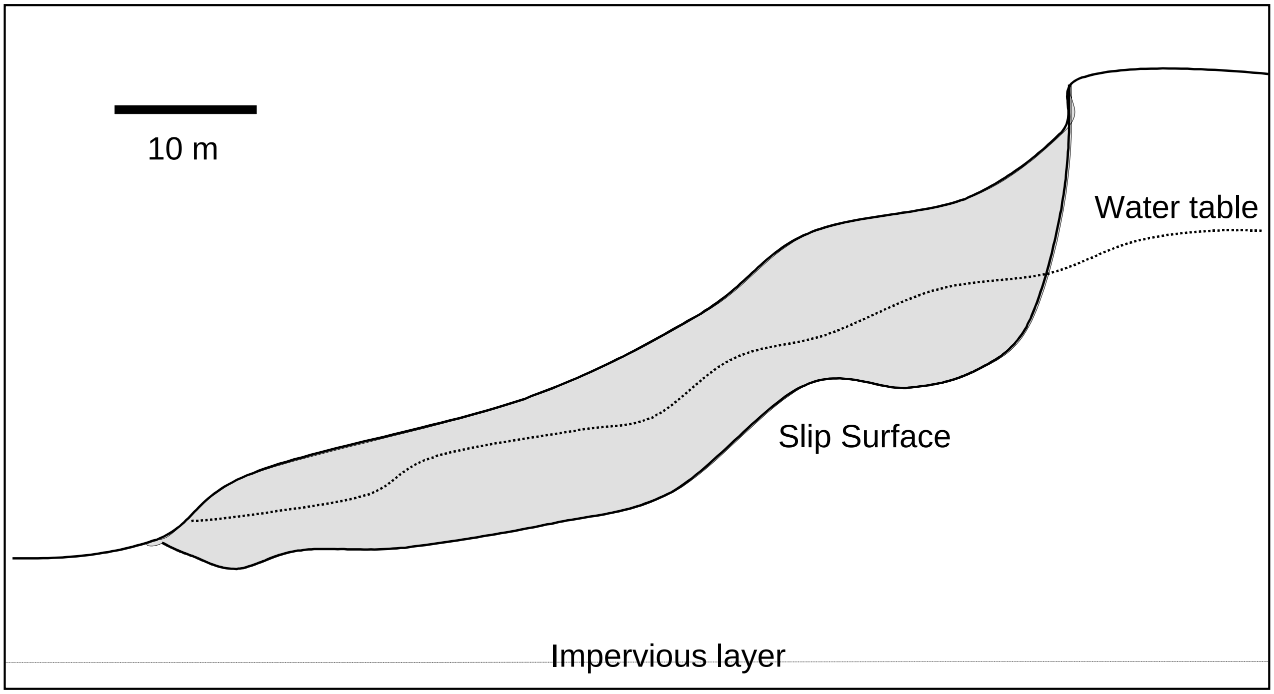

And the following average material properties:

- Average total unit weight = 20 kN/m^3
- Residual Cohesion = 5 kPa
- Residual Friction Angle = 15°

1. Calculate the average factor of safety, and the distribution of forces within the landslide. How sensitive is you solution to varying these parameters?
2. Assume that you have hydrostatic pore water conditions at the slip surface. How would you improve on this estimate of pore water pressure conditions
3. How would one have to either load or unload the upper ¼ of the slide in order to get a factor of safety of approximately 1.

PART II

1. Read the following paper:

   Baum, R.L., and Fleming, R.W., 1991. Use of longitudinal strain in identifying driving and resisting elements of landslides. *Geological Society of America Bulletin* **103**(8):1121-1132.

   A. What is the topic of the paper, and why is it important?

   B. How would you identify the various parts of the slide in surface mapping? Use information from some of the other papers we are reading in class. Cite references for your information.

   C. Using either the spreadsheet (janbu.xls) or programs (janbu31.cpp/janbu31.exe, janbu30.bas) provided perform a Janbu analysis of the Alani-Paty slide. Watch your coordinate system and slice numbering!

   D. What assumptions were made in the analysis of this slide? Are they reasonable?

   E. Would you perform a different analysis? If so, what would you do differently?

   F. Use infinite slope theory to analyze the Alani-Paty slide. How different is the factor of safety from that calculated using the Janbu method? Why do you think the results are similar/dissimilar?

   G. What would you do to stabilize the slide. Back this up with results from your analysis.

Appendix C. Computer Programs

Janbu31.cpp (18 pages)

Janbu30.bas (14 Pages)

Janbu.xls (8 pages)

Appendix D. Janbu (1973) Paper on *Slope Stability Computations*